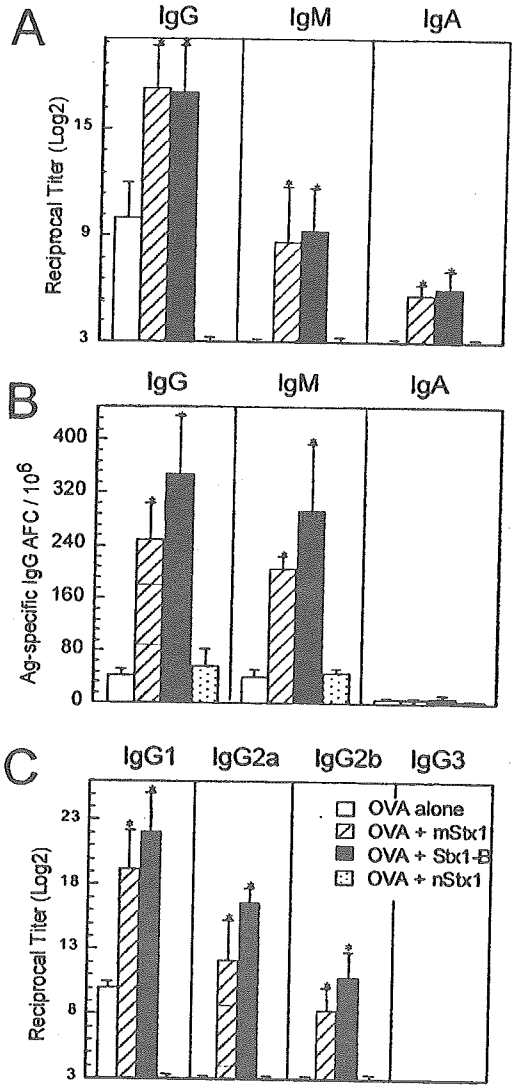

FIG. 3. Induction of OVA-specific antibody responses by coadministered Stx1 derivatives. Mice were subcutaneously immunized with OVA plus mStx1, nStx1, or StxB1. Specifically, C57BL/6 mice were subcutaneously immunized with 100 μg of OVA plus 10 μg of the Stx1 mutant (E167R/R170L; mStx1) (hatched bars), 50 ng of nStx1 (dotted bars), or 10 μg of StxB1 (black bars) as an adjuvant or with OVA alone (white bars) on days 0 and 14. OVA-specific serum IgG, IgM, and IgA Ab (A) and splenic OVA-specific antibody-forming cell (AFC) (B) responses were determined by ELISAs and ELISPOT assays, respectively. Furthermore, OVA-specific IgG subclass Ab responses (C) were also analyzed by ELISAs. Serum samples were collected on day 21 and examined for OVA-specific Abs and OVA-specific IgG subclass Ab responses by ELISAs. Mononuclear cells were isolated from the spleens of subcutaneously immunized mice on day 21 and examined by Ag-specific ELISPOT assays. *, $P < 0.05$ compared with mice immunized with OVA alone. The results are expressed as means ± SEM from a total of three separate experiments, each of which used five or six mice per group.

When $CD4^+$ T cells isolated from the spleens of mice subcutaneously immunized with OVA plus mStx1 or StxB1 were restimulated with OVA in vitro, increased proliferative responses were seen (Fig. 4A). In contrast, essentially no Ag-specific $CD4^+$ T-cell proliferation occurred in splenic $CD4^+$ T cells isolated from mice given OVA alone or OVA plus nStx1 (Fig. 4A). These results further demonstrate that mStx1 and StxB1 are potent adjuvants for the induction of OVA-specific $CD4^+$ T cells in vivo.

In a subsequent experiment, Th1 (IFN-γ) and Th2 (IL-4, IL-5, IL-6, and IL-10) cytokine production by antigen-specific $CD4^+$ T cells was analyzed at the protein level (Fig. 4B). Increased levels of both Th1 and Th2 cytokines were noted in cultures containing splenic $CD4^+$ T cells from mice subcutaneously immunized with OVA plus mStx1 or StxB1 (Fig. 4B), while nStx1 enhanced the production of only selected Th2 cytokines, including IL-5, IL-6, and IL-10, but not IL-4 and IFN-γ production (data not shown). Splenic $CD4^+$ T cells from mice given OVA alone produced low levels of IFN-γ, IL-5, IL-6, and IL-10 but did not produce IL-4. Taken together, these results show that the subcutaneous administration of OVA plus StxB1 or mStx1 as an adjuvant induces antigen-specific Th1 (e.g., IFN-γ)- and Th2 (e.g., IL-4)-type cytokine responses, which in turn account for the generation of OVA-specific IgG2a and IgG1 Ab responses, respectively, in serum.

Induction of neutralizing antibody responses to tetanus toxin by subcutaneous immunization with the toxoid vaccine and Stx1 derivatives. Since the subcutaneous administration of OVA plus mStx1 or StxB1 elicited Ag-specific IgG and IgM Ab responses, we next determined whether vaccine Ag-specific Abs supported by the Stx1 derivatives were protective. Initially, we determined whether the subcutaneous administration of tetanus toxoid (TT) with mStx1 or StxB1 could induce TT-specific Ab responses. Mice subcutaneously immunized with TT plus >10 μg of mStx1 or StxB1 showed significant TT-specific serum IgM, IgG, and IgA Ab responses. In contrast, low Ab responses were detected after immunization with TT alone (Fig. 5A). In the next experiment, we determined if these Abs were also protective. Mice given TT plus Stx1 derivatives or TT alone were challenged with a lethal dose (130 LD_{50}s) of tetanus toxin and then monitored for paralysis and death. As expected, subcutaneous immunization with TT plus Stx1 derivatives provided complete protection. In contrast, TT alone provided no protection in mice against the paralysis and death that normally occur within 2 days of the administration of tetanus toxin (Fig. 5B). These findings indicate the effectiveness of TT-specific IgG Abs in serum induced by subcutaneously coadministered Stx1 derivatives.

DISCUSSION

B7-1 and B7-2 have been shown to be essential costimulatory molecules for the initial activation of $CD4^+$ T cells (21, 23, 24). With our experiments, we sought to determine the effect of Stx1 derivatives on the expression of such costimulatory molecules. Immature BMDCs and splenic DCs were used to help map the early events occurring after the administration of Stx1 derivatives and to determine the extent of the ability of those derivatives to initiate primary T-cell responses. Stx1 derivatives provided two different types of immunoregulation signals to DCs. First, StxB1 and mStx1 were shown in our in vitro and in vivo studies to enhance the activation of BMDCs and splenic DCs by augmenting MHC class II, CD80, CD86,

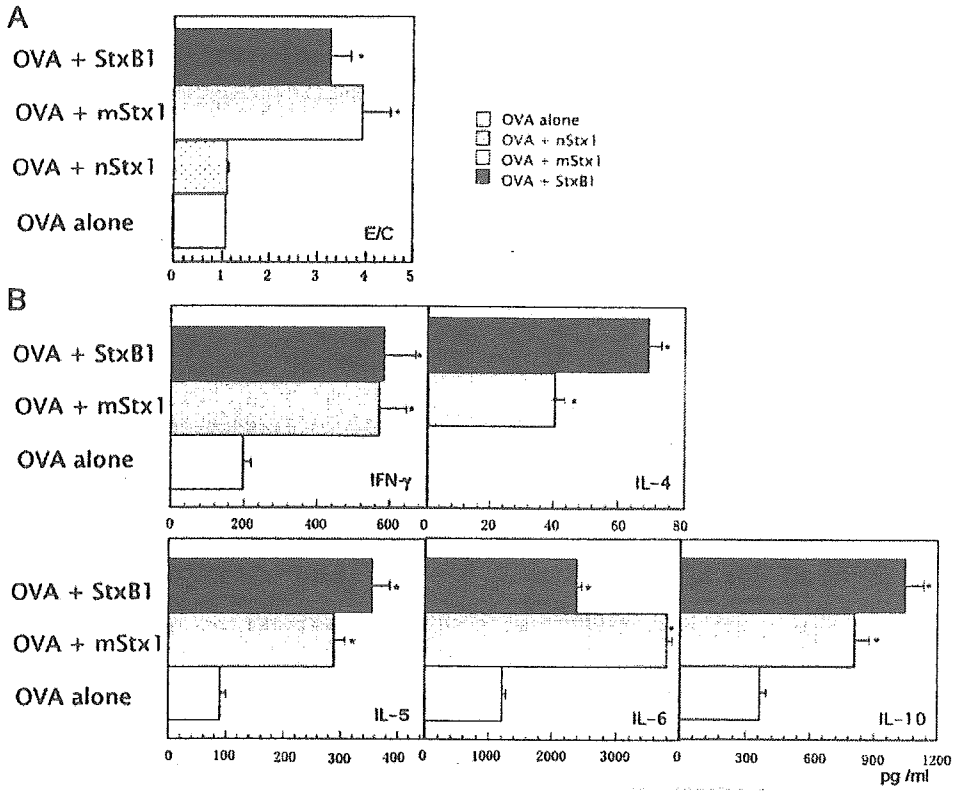

FIG. 4. Analysis of OVA-specific $CD4^+$ T-cell responses induced by coadministered Stx1 derivatives. OVA-specific $CD4^+$ Th-cell proliferative responses (A) and Th1 and Th2 cytokine synthesis (B) by $CD4^+$ T cells isolated from the spleens of mice subcutaneously immunized with OVA plus 10 μg of mStx1 (shaded bars), 50 ng of nStx1 (dotted bars), or 10 μg of StxB1 (black bars) or with OVA alone (white bars) were examined. Purified splenic $CD4^+$ T cells were cocultured at a density of 2×10^6 cells/ml with 1 mg/ml of OVA and with T-cell-depleted, irradiated splenic feeder cells (4×10^6 cells/ml) in complete medium containing rIL-2 (10 U/ml) for 3 days for proliferation assays and 5 days for cytokine synthesis measurements. A control culture consisting of the splenic $CD4^+$ T cells of naïve mice, feeder cells, and rIL-2 (10 U/ml) resulted in the incorporation of 230 ± 42 cpm of [^{3}H]thymidine. Culture supernatants were harvested and then analyzed for the synthesis of secreted cytokines by the use of appropriate cytokine-specific ELISAs. The minimum detection levels for the individual cytokines detected were as follows: IFN-γ, 9.4 pg/ml; IL-4, 7.8 pg/ml; IL-5, 15.6 pg/ml; IL-6, 15.6 pg/ml; and IL-10, 15.6 pg/ml. The results are expressed as means of the stimulation indexes ± SEM or pg/ml ± SEM from a total of three experiments using five or six mice per group. *, $P < 0.05$ compared with mice immunized with OVA alone. The results for OVA-specific $CD4^+$ T-cell proliferative responses (A) are expressed as E/C (experimental, stimulated value/control, nonstimulated value).

and/or CD40 expression. Since previous research has already shown that the strong expression of MHC and costimulatory molecules on antigen-presenting cells is associated with a high level of T-cell activation (4, 6), StxB1 and mStx1, with their demonstrated ability to enhance the expression of MHC and/or costimulatory molecules, must lead to an enhanced $CD4^+$ T-cell response. Second, certain Stx derivatives were shown to induce TNF-α, which has been shown to play a role in the immune regulation of B lymphocytes and the maturation of DCs (34, 49). Among the derivatives, StxB1 proved to be the most potent inducer of TNF-α. With the two distinct immunoenhancing signals noted above, nontoxic forms of Stx1 derivatives have been demonstrated by our study to be strong candidates as adjuvants to enhance antigen-specific T-cell and B-cell immune responses.

Our in vitro studies demonstrated that the maturation of in vitro BMDCs was enhanced by Stx1 derivatives, especially StxB1. Our results also showed that T-cell proliferation and cytokine production by Ag-specific $CD4^+$ T cells were augmented by StxB1-treated BMDCs. To examine whether the series of immunoenhancing events triggered by Stx1 derivative-treated BMDCs in vitro also reflected the in vivo situation, we also performed a series of in vivo experiments. Our findings revealed that DC maturation occurred after the administration of the Stx1 derivatives. Furthermore, we demonstrated that a mutant form of Stx1 (E167Q/R170L; mStx1) and the B subunit of Stx1 (StxB1) show potential as novel adjuvants for the induction of antigen-specific systemic Th and B-cell immune responses. The subcutaneous coadministration of nontoxic StxB1 or mStx1 as an adjuvant with a protein Ag resulted in the induction of high IgG anti-OVA Ab responses in serum. When these two distinct forms of nontoxic Stx1 derivatives were subcutaneously coadministered, the derivatives elicited both $CD4^+$ Th1- and Th2-type responses via the mixed production of Th1 (IFN-γ) and Th2 (IL-4, IL-5, IL-6, and IL-10) cytokines. The Stx1 derivative supported mixed (Th1 and Th2) cytokine synthesis, reflecting the generation of OVA-specific IgG1, followed by IgG2a, in the systemic compartment. Similarly, Stx1 derivative molecules were seen to support the generation of Ag-specific Th1- and Th2-type $CD4^+$ T cells in vitro.

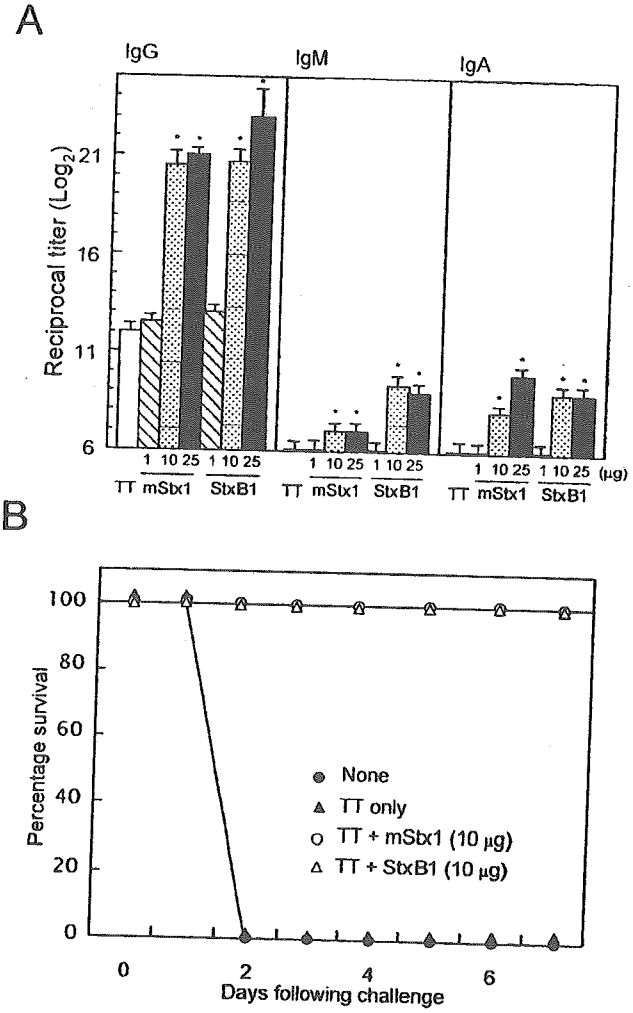

FIG. 5. Induction of TT-specific serum IgG, IgM, and IgA antibody responses by coadministered Stx1 derivatives (A) and protection against fatal challenge with tetanus toxin (B). Mice were subcutaneously immunized with TT plus mStx1, nStx1, or StxB1. Specifically, C57BL/6 mice were subcutaneously immunized with 100 μl of TT plus 1 μg of Stx1 mutant (E167R/R170L; mStx1) or 1 μg of StxB1 (hatched bars), 10 μg of Stx1 mutant or 10 μg of StxB1 (dotted bars), or 25 μg of Stx1 mutant or 25 μg of StxB1 (black bars) as an adjuvant or with TT alone (white bars) on days 0 and 14. Serum samples were collected on day 21 and examined for TT-specific Ab responses by ELISA. One week after the last immunization, mice were challenged on day 21 by the subcutaneous injection of 130 LD_{50}s of tetanus toxin in 0.5 ml of PBS including 0.2% gelatin. *, $P < 0.05$ compared with mice immunized with OVA alone. The results are expressed as means ± SEM from a total of three separate experiments, each of which used five or six mice per group.

In addition to Stx1 derivatives, pertussis toxin (37) and LT (47) have been shown to potentiate a similarly mixed Th1- and Th2-type response.

In a separate study, LT-treated BMDCs, like StxB1-treated cells, were shown to enhance CD80, CD86, MHC class II, and CD40 expression (unpublished data). It has been shown that the up-regulation of CD80, CD86, MHC class II, or TNF-α and/or IL-12 production most closely correlates with the adjuvant activity of toxin-based immunomodulatory molecules (8, 53). Although many details of the molecular mechanisms behind the enhancement of Th1- and Th2-type responses by Stx derivatives remain to be elucidated, the present study has demonstrated that the Stx derivatives (e.g., StxB1 and mStx1) can be grouped as Th1- and Th2-inducing adjuvants. For an investigation of the molecular mechanisms underlying the adjuvanticity of mStx1 and StxB1, one possible experiment would be to examine and compare the Th1- and Th2-type pathway induced by mStx1 and that promoted by StxB1. The induction of signaling molecules such as T-bet, GATA-3, c-Maf, and SLAT by mStx1 and StxB1 could be compared, since these molecules have been shown to be associated with Th1- or Th2-cell differentiation (19, 27, 46).

Our results revealed that 50 ng of nStx1 did not induce serum IgG Ab responses to a coadministered Ag, indicating that nStx1 does not possess adjuvant activity. This observation is consistent with a previous study that showed that nStx1 does not possess adjuvant activity when given orogastrically (43). In contrast, all mice given 10 μg of mStx1 or StxB1 as an adjuvant generated systemic antigen-specific IgG responses (Fig. 4). Since a lower concentration of nStx1 was used in the in vivo experiment, one can consider that the administration of a higher dose may lead to the induction of the antigen-specific immune responses seen with mStx1 and StxB1. To this end, we subcutaneously coadministered higher doses of nStx1 (e.g., 100 to 150 ng) to mice, and all of those mice died (data not shown). These findings further demonstrate that nontoxic forms such as mStx1 and StxB1 possess adjuvant activities when administered at high doses, while the adjuvanticity of the native form cannot be assessed at these high doses due to its toxicity. In addition, mStx1 and StxB1 do not have the damaging side effects of nStx1. Previous studies have reported that Stxs induce necrosis via their RNA *N*-glycosidase activity (39) but that, in contrast, the Stx1 mutant and StxB1 (2) are much less toxic or nontoxic in terms of their inhibitory effects on protein synthesis, their cytotoxicity, and their lethality to mice compared with native forms of Stx1 (2, 33). nStx1 may signal the induction of cell death instead of immune enhancement. In contrast, the nontoxic forms, mStx1 and StxB1, provide appropriate activation signals for the induction of $CD4^+$ Th1- and Th2-type responses via the expression of CD80, CD86, and MHC class II on DCs, leading to the generation of IgG1 and IgG2a Ab responses to the coadministered Ag.

It is well established that CT is an effective adjuvant for the induction of antigen-specific mucosal IgA and systemic IgG and IgA Ab responses to coadministered protein Ags (9). CT preferentially induces Ag-specific Th2-type $CD4^+$ T-cell responses via the high-level synthesis of IL-4 and IL-5 (28). However, the enterotoxin possesses ADP-ribosyltransferase activity, which causes severe diarrhea and is thus unsuitable for use in humans (41). Therefore, several studies have investigated the potential adjuvant effect of the B subunit as a nontoxic derivative of CT. Highly purified recombinant CT-B has been shown to be ineffective as an adjuvant compared with the holotoxin for the induction of Ag-specific IgA and IgG immune responses (25, 54). However, it should be noted that two recent studies provided contradictory results, showing that nasally coadministered recombinant CT-B provided mucosal adjuvant activity (13, 48). It is interesting that StxB1 possesses adjuvant activity. Since the membrane ligand molecules of

StxB1 (e.g., globotriaosylceramid [Gb3] and globotetraosylceramide [Gb4]) are completely different from those of CT-B and LT-B (e.g., GM1), biological stimulation signals provided by StxB1 via Gb3 and Gb4 could be more effective than those transmitted by CT-B and GM1. Several cell surface receptors, including Ig, transferrin receptor, FcγR, and DEC-205, can mediate endocytosis and effective antigen presentation (16, 29, 35). Furthermore, glycosphingolipids, including GM1, have also been implicated as sites for the delivery of immunity-enhancing signals (40). Our present findings suggest that Gb3 may also mediate the effective endocytosis of and antigen presentation by DCs. Therefore, the A subunits of the toxins may not be necessary for immunoenhancing activity, unlike those of other known AB_5 toxins such as CT and LT. In this study, StxB1 possessed a costimulatory molecule-enhancing activity, while CT-B fails to induce either CD80 or CD86 expression on B cells or macrophages (1, 53). To elucidate the relationship between the increased expression of costimulatory molecules and the binding of StxB1 to its receptor, Gb3, we examined whether the signals for the enhancement of costimulatory molecules by StxB1 can be blocked by treatment of the receptors for StxB1. After a treatment of Gb3, costimulatory molecule expression was blocked (unpublished data). This means that the signaling pathway via the receptor for StxB1 plays a role in the enhancement of costimulatory molecule expression. In addition, it should be noted that it is possible that the A subunit of Stx1 is more responsible for toxicity than for adjuvanticity.

The nStx1 treatment of BMDCs was associated with some increase in OVA-specific $CD4^+$ T-cell proliferative as well as Th1/Th2 cytokine responses (Fig. 2). However, nStx1 did not induce any up-regulation of CD80, CD86, or MHC class II and did not enhance the secretion of TNF-α or IL-12 (Fig. 1 and Table 1). When the nStx1-treated BMDCs were treated with CD80- and/or CD86-blocking antibodies, the levels of $CD4^+$ T-cell proliferation and Th1/Th2 cytokine secretion were not altered. However, when mStx1- or StxB1-treated BMDCs were similarly treated with blocking antibodies specific for CD80 and CD86, the antigen-specific $CD4^+$ T-cell responses were inhibited (unpublished results). These findings suggest that the ability of nStx1 to stimulate the proliferation and cytokine secretion of T cells does not stem from the up-regulation of costimulatory molecules.

Another interesting biological characteristic of nStx1 is that its in vivo administration resulted in the down-regulation of all of the surface molecules associated with lymphocyte stimulation on splenic DCs (Table 2). To this end, nStx2 has been shown to reduce the number of splenic $CD4^+$ and $B220^+$ cells when it is administered to mice (44). Thus, nStx1 may exert at least two negative influences on lymphocytes, namely, it can down-regulate costimulatory molecule expression or even result in death. A separate study lent support to this view by showing that approximately 25% of BMDCs underwent apoptosis and necrosis after exposure to nStx1 in vitro, while no such cell death was seen after exposure to nontoxic Stx1 derivatives such as mStx1 and StxB1 (data not shown).

In summary, our findings have provided new evidence that nontoxic Stx1 derivatives (e.g., mStx1 and StxB1) can effectively induce costimulatory molecules (CD80 and CD86) and/or MHC class II on DCs. This study has further shown that nontoxic forms of Stx1 derivatives, including mStx1 and StxB1, possess adjuvant activity and can elicit Ag-specific $CD4^+$ Th1- and Th2-type responses for the subsequent induction of antigen-specific IgG1 and IgG2a Ab responses following subcutaneous immunization with a protein Ag. The nontoxic Stx derivatives can be considered promising new candidates for effective and safe adjuvants.

ACKNOWLEDGMENTS

We appreciate the constructive comments regarding this work by members of the Division of Immunology and Medical Zoology of Niigata University Graduate School of the Medical and Dental Sciences and the Department of Mucosal Immunology of the Research Institute for Microbial Diseases, Osaka University.

This study was supported by grants from the Ministry of Health, Labor and Welfare; the Ministry of Education, Science, Sports and Culture; and CREST, JST; and the Research Institute of Oral Sciences, Nihon University School of Dentistry at Matsuda, Japan. M.O. was supported by the Japan Human Health Science Foundation.

All experiments described herein were approved by the local authorities. All procedures were done in agreement with National Institutes of Health guidelines for the handling of laboratory animals.

REFERENCES

1. **Agren, L. C., L. Ekman, B. Lowenadler, and N. Y. Lycke.** 1997. Genetically engineered nontoxic vaccine adjuvant that combines B cell targeting with immunomodulation by cholera toxin A1 subunit. J. Immunol. **158**:3936–3946.
2. **Austin, P. R., and C. J. Hovde.** 1995. Purification of recombinant Shiga-like toxin type I B subunit. Protein Expr. Purif. **6**:771–779.
3. **Birnabaum, S., and M. Pinto.** 1976. Local and systemic opsonic adherent, hemagglutinating and rosette forming activity in mice induced by respiratory immunization with sheep red blood cells. Z. Immunitatsforsch. Exp. Klin. Immunol. **151**:69–77.
4. **Bluestone, J. A.** 1995. New perspectives of CD28-B7-mediated T cell costimulation. Immunity **2**:555–559.
5. **Byun, Y., M. Ohmura, K. Fujihashi, S. Yamamoto, J. McGhee, S. Udaka, H. Kiyono, Y. Takeda, T. Kohsaka, and Y. Yuki.** 2001. Nasal immunization with *E. coli* verotoxin 1 (VT1)-B subunit and a nontoxic mutant of cholera toxin elicits serum neutralizing antibodies. Vaccine **19**:2061–2070.
6. **Cella, M., F. Sallusto, and A. Lanzavecchia.** 1997. Origin, maturation and antigen presenting function of dendritic cells. Curr. Opin. Immunol. **9**:10–16.
7. **Clements, J. D., N. M. Hartzog, and F. L. Lyon.** 1988. Adjuvant activity of *Escherichia coli* heat-labile enterotoxin and effect on the induction of oral tolerance in mice to unrelated protein antigens. Vaccine **6**:269–277.
8. **Cong, Y., C. T. Weaver, and C. O. Elson.** 1997. The mucosal adjuvanticity of cholera toxin involves enhancement of costimulatory activity by selective up-regulation of B7.2 expression. J. Immunol. **159**:5301–5308.
9. **Elson, C. O., and W. Ealding.** 1984. Generalized systemic and mucosal immunity in mice after mucosal stimulation with cholera toxin. J. Immunol. **132**:2736–2741.
10. **Endo, Y., K. Tsurigi, T. Yutsudo, Y. Takeda, T. Ogasawara, and K. Igarashi.** 1988. Site of action of a Vero toxin (VT2) from *Escherichia coli* O157:H7 and of Shiga toxin on eukaryotic ribosomes. RNA N-glycosidase activity of the toxins. Eur. J. Biochem. **171**:45–50.
11. **Herzenberg, L. A., T. Tokuhisa, and D. R. Parks.** 1982. Epitope-specific regulation. II. A bistable, Igh-restricted regulatory mechanism central to immunologic memory. J. Exp. Med. **155**:1741–1753.
12. **Inaba, K., M. Inaba, N. Romani, H. Aya, M. Deguchi, S. Ikehara, S. Muramatsu, and R. M. Steinman.** 1992. Generation of large numbers of dendritic cells from mouse bone marrow cultures supplemented with granulocyte/macrophage colony-stimulating factor. J. Exp. Med. **176**:1693–1702.
13. **Isaka, M., Y. Yasuda, S. Kozuka, T. Taniguchi, K. Matano, J. Maeyama, T. Komiya, K. Ohkuma, N. Goto, and K. Tochikubo.** 1999. Induction of systemic and mucosal antibody responses in mice immunized intranasally with aluminium-non-adsorbed diphtheria toxoid together with recombinant cholera toxin B subunit as an adjuvant. Vaccine **18**:743–751.
14. **Ito, H., T. Yutsudo, T. Hirayama, and Y. Takeda.** 1988. Isolation and some properties of A and B subunits of Vero toxin 2 and in vitro formation of hybrid toxins between subunits of Vero toxin 1 and Vero toxin 2 from *Escherichia coli* O157:H7. Microb. Pathog. **5**:189–195.
15. **Jackson, R. J., K. Fujihashi, J. Xu-Amano, H. Kiyono, C. O. Elson, and J. R. McGhee.** 1993. Optimizing oral vaccines: induction of systemic and mucosal B-cell and antibody responses to tetanus toxoid by use of cholera toxin as an adjuvant. Infect. Immun. **61**:4272–4279.
16. **Jiang, W., W. J. Swiggard, C. Heufler, M. Peng, A. Mirza, R. M. Steinman, and M. C. Nussenzweig.** 1995. The receptor DEC-205 expressed by dendritic

cells and thymic epithelial cells is involved in antigen processing. Nature 375:151–155.
17. **Kaisho, T., O. Takeuchi, T. Kawai, K. Hoshino, and S. Akira.** 2001. Endotoxin-induced maturation of MyD88-deficient dendritic cells. J. Immunol. 166:5688–5694.
18. **Katz, J. M., X. Lu, S. A. Young, and J. C. Galphin.** 1997. Adjuvant activity of the heat-labile enterotoxin from enterotoxigenic *Escherichia coli* for oral administration of inactivated influenza virus vaccine. J. Infect. Dis. 175:352–363.
19. **Kuo, C. T., and J. M. Leiden.** 1999. Transcriptional regulation of T lymphocyte development and function. Annu. Rev. Immunol. 17:149–187.
20. **Kweon, M. N., M. Yamamoto, F. Watanabe, S. Tamura, F. W. Van Ginkel, A. Miyauchi, H. Takagi, Y. Takeda, T. Hamabata, K. Fujihashi, J. R. McGhee, and H. Kiyono.** 2002. A nontoxic chimeric enterotoxin adjuvant induces protective immunity in both mucosal and systemic compartments with reduced IgE antibodies. J. Infect. Dis. 186:1261–1269.
21. **Lanier, L. L., S. O'Fallon, C. Somoza, J. H. Phillips, P. S. Linsley, K. Okumura, D. Ito, and M. Azuma.** 1995. CD80 (B7) and CD86 (B70) provide similar costimulatory signals for T cell proliferation, cytokine production, and generation of CTL. J. Immunol. 154:97–105.
22. **Larsson, R., D. Rocksen, B. Lilliehook, A. Jonsson, and A. Bucht.** 2000. Dose-dependent activation of lymphocytes in endotoxin-induced airway inflammation. Infect. Immun. 68:6962–6969.
23. **Lenschow, D. J., S. C. Ho, H. Sattar, L. Rhee, G. Gray, N. Nabavi, K. C. Herold, and J. A. Bluestone.** 1995. Differential effects of anti-B7-1 and anti-B7-2 monoclonal antibody treatment on the development of diabetes in the nonobese diabetic mouse. J. Exp. Med. 181:1145–1155.
24. **Lenschow, D. J., T. L. Walunas, and J. A. Bluestone.** 1996. CD28/B7 system of T cell costimulation. Annu. Rev. Immunol. 14:233–258.
25. **Lycke, N., T. Tsuji, and J. Holmgren.** 1992. The adjuvant effect of *Vibrio cholerae* and *Escherichia coli* heat-labile enterotoxins is linked to their ADP-ribosyltransferase activity. Eur. J. Immunol. 22:2277–2281.
26. **Macatonia, S. E., S. C. Knight, A. J. Edwards, S. Griffiths, and P. Fryer.** 1987. Localization of antigen on lymph node dendritic cells after exposure to the contact sensitizer fluorescein isothiocyanate. Functional and morphological studies. J. Exp. Med. 166:1654–1667.
27. **Madrenas, J.** 2003. A SLAT in the Th2 signalosome. Immunity 18:459–461.
28. **Marinaro, M., H. F. Staats, T. Hiroi, R. J. Jackson, M. Coste, P. N. Boyaka, N. Okahashi, M. Yamamoto, H. Kiyono, H. Bluethmann, et al.** 1995. Mucosal adjuvant effect of cholera toxin in mice results from induction of T helper 2 (Th2) cells and IL-4. J. Immunol. 155:4621–4629.
29. **McCoy, K. L., M. Noone, J. K. Inman, and R. Stutzman.** 1993. Exogenous antigens internalized through transferrin receptors activate $CD4^+$ T cells. J. Immunol. 150:1691–1704.
30. **Mrsny, R. J., A. L. Daugherty, C. M. Fryling, and D. J. FitzGerald.** 1999. Mucosal administration of a chimera composed of Pseudomonas exotoxin and the gp120 V3 loop sequence of HIV-1 induces both salivary and serum antibody responses. Vaccine 17:1425–1433.
31. **Murphy, K. M., A. B. Heimberger, and D. Y. Loh.** 1990. Induction by antigen of intrathymic apoptosis of $CD4^+$,$CD8^+TCR^{lo}$ thymocytes in vivo. Science 250:1720–1723.
32. **Northrup, R. S., and A. S. Fauci.** 1972. Adjuvant effect of cholera enterotoxin on the immune response of the mouse to sheep red blood cells. J. Infect. Dis. 125:672–673.
33. **Ohmura, M., S. Yamasaki, H. Kurazono, K. Kashiwagi, K. Igarashi, and Y. Takeda.** 1993. Characterization of non-toxic mutant toxins of Vero toxin 1 that were constructed by replacing amino acids in the A subunit. Microb. Pathog. 15:169–176.
34. **Pasparakis, M., L. Alexopoulou, V. Episkopou, and G. Kollias.** 1996. Immune and inflammatory responses in TNF alpha-deficient mice: a critical requirement for TNF alpha in the formation of primary B cell follicles, follicular dendritic cell networks and germinal centers, and in the maturation of the humoral immune response. J. Exp. Med. 184:1397–1411.
35. **Regnault, A., D. Lankar, V. Lacabanne, A. Rodriguez, C. Thery, M. Rescigno, T. Saito, S. Verbeek, C. Bonnerot, P. Ricciardi-Castagnoli, and S. Amigorena.** 1999. Fc gamma receptor-mediated induction of dendritic cell maturation and major histocompatibility complex class I-restricted antigen presentation after immune complex internalization. J. Exp. Med. 189:371–380.
36. **Roberts, M., A. Bacon, R. Rappuoli, M. Pizza, I. Cropley, G. Douce, G. Dougan, M. Marinaro, J. McGhee, and S. Chatfield.** 1995. A mutant pertussis toxin molecule that lacks ADP-ribosyltransferase activity, PT-9K/129G, is an effective mucosal adjuvant for intranasally delivered proteins. Infect. Immun. 63:2100–2108.
37. **Ryan, M., L. McCarthy, R. Rappuoli, B. P. Mahon, and K. H. Mills.** 1998. Pertussis toxin potentiates Th1 and Th2 responses to co-injected antigen: adjuvant action is associated with enhanced regulatory cytokine production and expression of the co-stimulatory molecules B7-1, B7-2 and CD28. Int. Immunol. 10:651–662.
38. **Samuel, J. E., L. P. Perera, S. Ward, A. D. O'Brien, V. Ginsburg, and H. C. Krivan.** 1990. Comparison of the glycolipid receptor specificities of Shiga-like toxin type II and Shiga-like toxin type II variants. Infect. Immun. 58:611–618.
39. **Saxena, S. K., A. D. O'Brien, and E. J. Ackerman.** 1989. Shiga toxin, Shiga-like toxin II variant, and ricin are all single-site RNA N-glycosidases of 28S RNA when microinjected into *Xenopus* oocytes. J. Biol. Chem. 264:596–601.
40. **Simons, K., and E. Ikonen.** 1997. Functional rafts in cell membranes. Nature 387:569–572.
41. **Spangler, B. D.** 1992. Structure and function of cholera toxin and the related *Escherichia coli* heat-labile enterotoxin. Microbiol. Rev. 56:622–647.
42. **Stockbine, N., L. Marques, J. Newland, H. Smith, R. Holmes, and A. O'Brien.** 1986. Two toxin-converting phages from *Escherichia coli* O157:H7 strain 933 encode antigenically distinct toxins with similar biologic activities. Infect. Immun. 53:135–140.
43. **Suckow, M. A., D. F. Keren, J. E. Brown, and G. T. Keusch.** 1994. Stimulation of gastrointestinal antibody to Shiga toxin by orogastric immunization in mice. Immunol. Cell Biol. 72:69–74.
44. **Sugatani, J., T. Igarashi, M. Shimura, T. Yamanaka, T. Takeda, and M. Miwa.** 2000. Disorders in the immune responses of T- and B-cells in mice administered intravenous verotoxin 2. Life Sci. 67:1059–1072.
45. **Swiggard, W., M. D. Noncas, M. D. Witmer-Pack, and R. M. Steinman.** 1991. Enrichment of dendritic cells by plastic adherence and EA resetting, p. 3.7.1–3.7.11. *In* J. E. Coligan (ed.), Current protocols in immunology. John Wiley & Sons, Inc., New York, N.Y.
46. **Szabo, S. J., S. T. Kim, G. L. Costa, X. Zhang, C. G. Fathman, and L. H. Glimcher.** 2000. A novel transcription factor, T-bet, directs Th1 lineage commitment. Cell 100:655–669.
47. **Takahashi, I., M. Marinaro, H. Kiyono, R. J. Jackson, I. Nakagawa, K. Fujihashi, S. Hamada, J. D. Clements, K. L. Bost, and J. R. McGhee.** 1996. Mechanisms for mucosal immunogenicity and adjuvancy of *Escherichia coli* labile enterotoxin. J. Infect. Dis. 173:627–635.
48. **Tochikubo, K., M. Isaka, Y. Yasuda, S. Kozuka, K. Matano, Y. Miura, and T. Taniguchi.** 1998. Recombinant cholera toxin B subunit acts as an adjuvant for the mucosal and systemic responses of mice to mucosally co-administered bovine serum albumin. Vaccine 16:150–155.
49. **Trevejo, J. M., M. W. Marino, N. Philpott, R. Josien, E. C. Richards, K. B. Elkon, and E. Falck-Pedersen.** 2001. TNF-alpha-dependent maturation of local dendritic cells is critical for activating the adaptive immune response to virus infection. Proc. Natl. Acad. Sci. USA 98:12162–12167.
50. **Ultrich, J. T., J. L. Cantrell, G. L. Gustafson, J. A. Rudbach, and J. R. Hiernant.** 1991. The adjuvant activity of monophosphoryl lipid A. CRC Press, Boca Raton, Fla.
51. **VanCott, J. L., H. F. Staats, D. W. Pascual, M. Roberts, S. N. Chatfield, M. Yamamoto, M. Coste, P. B. Carter, H. Kiyono, and J. R. McGhee.** 1996. Regulation of mucosal and systemic antibody responses by T helper cell subsets, macrophages, and derived cytokines following oral immunization with live recombinant Salmonella. J. Immunol. 156:1504–1514.
52. **Xu-Amano, J., H. Kiyono, R. J. Jackson, H. F. Staats, K. Fujihashi, P. D. Burrows, C. O. Elson, S. Pillai, and J. R. McGhee.** 1993. Helper T cell subsets for immunoglobulin A responses: oral immunization with tetanus toxoid and cholera toxin as adjuvant selectively induces Th2 cells in mucosa associated tissues. J. Exp. Med. 178:1309–1320.
53. **Yamamoto, M., H. Kiyono, S. Yamamoto, E. Batanero, M. N. Kweon, S. Otake, M. Azuma, Y. Takeda, and J. R. McGhee.** 1999. Direct effects on antigen-presenting cells and T lymphocytes explain the adjuvanticity of a nontoxic cholera toxin mutant. J. Immunol. 162:7015–7021.
54. **Yamamoto, S., H. Kiyono, M. Yamamoto, K. Imaoka, K. Fujihashi, F. W. Van Ginkel, M. Noda, Y. Takeda, and J. R. McGhee.** 1997. A nontoxic mutant of cholera toxin elicits Th2-type responses for enhanced mucosal immunity. Proc. Natl. Acad. Sci. USA 94:5267–5272.
55. **Yamamoto, S., Y. Takeda, M. Yamamoto, H. Kurazono, K. Imaoka, K. Fujihashi, M. Noda, H. Kiyono, and J. R. McGhee.** 1997. Mutants in the ADP-ribosyltransferase cleft of cholera toxin lack diarrheagenicity but retain adjuvanticity. J. Exp. Med. 185:1203–1210.

Editor: J. T. Barbieri

Prenatal Blockage of Lymphotoxin β Receptor and TNF Receptor p55 Signaling Cascade Resulted in the Acceleration of Tissue Genesis for Isolated Lymphoid Follicles in the Large Intestine[1]

Mi-Na Kweon,[2*†] Masafumi Yamamoto,[†‡] Paul D. Rennert,[§] Eun Jeong Park,[†] Ah-Young Lee,[*] Sun-Young Chang,[*] Takachika Hiroi,[†] Masanobu Nanno,[¶] and Hiroshi Kiyono[†‖]

Signaling by lymphotoxin (LT) and TNF is essential for the organogenesis of secondary lymphoid tissues in systemic and mucosal compartments. In this study, we demonstrated that the progeny of mice treated with fusion protein of LTβR and IgGFc (LTβR-Ig) or LTβR-Ig plus TNFR55-Ig (double Ig) showed significantly increased numbers of isolated lymphoid follicles (ILF) in the large intestine. Interestingly, double Ig treatment accelerated the maturation of large intestinal ILF. Three-week-old progeny of double Ig-treated mice showed increased numbers of ILF in the large intestine, but not in the small intestine. Furthermore, alteration of intestinal microflora by feeding of antibiotic water did not affect the increased numbers of ILF in the large intestine of double Ig-treated mice. Most interestingly, mice that developed numerous ILF also had increased levels of activation-induced cytidine deaminase expression and numbers of IgA-expressing cells in the lamina propria of the large intestine. Taken together, these results suggest that ILF formation in the large intestine is accelerated by blockage of LTβR and TNFR55 signals in utero, and ILF, like colonic patches, might play a role in the induction of IgA response in the large intestine. ***The Journal of Immunology,*** **2005, 174: 4365–4372.**

The gut-associated lymphoid tissues are characterized as the initiation sites for the induction of IgA-mediated immunity and mucosally induced tolerance (1, 2). The mucosal immune system possesses a network of lymphoid organs that are composed of inductive sites (e.g., Peyer's patches (PP))[3] and effector sites (the intraepithelial and the lamina propria (LP) region) (1, 2). It had been believed that PP is the major inductive site for the initiation of Ag-specific IgA responses to a variety of exogenous Ag (3, 4); however, we and others have demonstrated that PP contribute to, but are not essential for, the induction of Ag-specific mucosal IgA responses (5–7). A recent study revealed the existence of isolated lymphoid follicles (ILF) in the small intestine that resemble PP in terms of architecture and cellular composition (8). The fact that ILF possess germinal centers and an overlying follicle-associated epithelium (FAE) containing M cells suggests their possible role as mucosal inductive sites (8).

Lymphotoxin (LT), a TNF family member, can be found in two forms: a membrane-bound heterotrimer and a soluble homotrimer (9, 10). The membrane-bound heterotrimer is comprised of two β-chains and one α-chain (LTα1β2) and is a ligand for LTβR, while the soluble homotrimer (LTα3) is ligand for both TNFR55 and TNFR75 (11, 12). Unlike the LTα trimer and TNF, which are secreted proteins, LTαβ remains membrane bound and is expressed on the restricted hemopoietic lineage, particularly by T cells, B cells, and NK cells (13). The interaction of LTαβ with LTβR is the critical molecular event triggering secondary lymphoid organ genesis and controlling spleen organization. For example, congenital lack of LTα, LTβ, or LTβR genes disrupted PP and lymph node (LN) organogenesis, and altered splenic architecture as characterized by the absence of distinct T and B cell areas and disruption of the marginal zone (14–17). Furthermore, administration of LTβR-Ig fusion protein to mice during the selected time window of embryogenesis disrupted LN and PP formation in the progeny (18, 19), suggesting that the molecular interaction of membrane-bound LT with LTβR during the gestational period is essential for the initiation of LN and PP development. In contrast to PP, a recent study demonstrated that ILF formation was not influenced by the blockage of LTβR signaling with LTβR-Ig fusion protein during gestation (8). However, no ILF was found in $LT\alpha^{-/-}$ or *aly/aly* mice, implying that ILF do require signals dependent on LT and NF-κB-inducing kinase, a critical downstream signaling molecule associated with LTβR, postgestation (8). It has recently been confirmed that, unlike PP formation, ILF formation requires LT-LTβR interaction in adulthood, as well as TNFR55-mediated signaling for their maturation (20).

*Mucosal Immunology Section, International Vaccine Institute, Seoul, Korea; †Division of Mucosal Immunology, Institute of Medical Science, University of Tokyo, Tokyo, Japan; ‡Department of Oral Medicine, Nihon University School of Dentistry at Masudo, Matsudo, Chiba, Japan; §Department of Immunology and Inflammation, Biogen-Idec, Cambridge, MA 02142; ¶Yakult Central Institute for Microbiological Research, Tokyo, Japan; and ‖Core Research for Engineering, Science, and Technology, Japan Science Technology, Tokyo, Japan

Received for publication February 12, 2004. Accepted for publication January 26, 2005.

The costs of publication of this article were defrayed in part by the payment of page charges. This article must therefore be hereby marked *advertisement* in accordance with 18 U.S.C. Section 1734 solely to indicate this fact.

[1] This work is supported by grants from Core Research for Engineering, Science, and Technology of Japan Science and Technology Agency; the Ministry of Education, Science, Sports, and Culture; and the Ministry of Health and Welfare in Japan; and supported by Special Coordination Funds of the Ministry of Education, Culture, Sports, Science, and Technology; the Japanese Government; as well as a Science Research Center fund to the Immunomodulation Center at University of Ulsan from the Korean Science Engineering Foundation and the Korean Ministry of Science and Technology.

[2] Address correspondence and reprint requests to Dr. Mi-Na Kweon, Mucosal Immunology Section, International Vaccine Institute, Seoul National University Research Park, Kwanak-Gu, Seoul, Korea 151-818. E-mail address: mnkweon@ivi.int

[3] Abbreviations used in this paper: PP, Peyer's patch; AID, activation-induced cytidine deaminase; CP, colonic patch; FAE, follicle-associated epithelium; ILF, isolated lymphoid follicle; LI-ILF, large intestinal ILF; LN, lymph node; LP, lamina propria; LT, lymphotoxin; PNA, peanut agglutinin.

0022-1767/05/$02.00

An additional component of the gut immune system is the colonic patch (CP). The cytoarchitectural components and immune functions of CP and PP were remarkably similar, despite differences in the surrounding environment of mucosa and luminal microbial exposure (21). The presence of organized lymphoid tissue with M cells and germinal centers in CP suggests that Ag uptake and recognition can take place in the rectum (22, 23). Similar to the PP, in utero treatment with LTβR-Ig fusion protein depleted CP formation in progeny (23). These results suggested that PP and CP were developmentally and functionally related components of the small intestine and large intestinal (colonic) immune systems, respectively. In addition to CP, it was shown that ~50 ILF were dispersed throughout the large intestine of BALB/c mice (8). Recently, it was reported that in utero treatment of mice with LTβR-Ig and TNFR55-Ig fusion proteins caused an increase in the number of submucosal lymphoid patches in the large intestine (24). This suggests that ILF in the small and large intestine are developmentally similar, although little else is known about these immunological structures and functions. In particular, the function of ILF in the large intestine and the precise contribution of LTβR and TNFR55 for their genesis, maturation, and the subsequent induction of IgA responses remain to be elucidated.

In this study, we provide several new findings regarding the unique contribution of the inflammatory cytokines LT and TNF in the genesis and function of ILF in the large intestine. In particular, the tissue genesis signals provided by the cytokine receptors of LTβR and TNFR55 are essential for the postnatal development of large intestinal ILF (LI-ILF). Our present findings suggest that the receptors behave as negative regulators for the genesis of LI-ILF because the blockage of prenatal LT/LTβR and TNF/TNFR55 signaling cascades accelerated the formation and maturation of ILF in the large intestine. Secondly, environmental factors, such as microflora-associated Ags, did not affect the formation and maturation of ILF in the large intestine. Finally, ILF in the large intestine play an important role for IgA^+ B cell development.

Materials and Methods

Mice

Timed pregnant BALB/c mice were purchased from Japan CLEA. These mice were maintained in the experimental facility under pathogen-free conditions in the Research Institute for Microbial Diseases at Osaka University and International Vaccine Institute and received sterilized food (certified diet MF; Oriental Yeast) and tap water ad libitum. TNF and LTα double-knockout ($TNF/LT\alpha^{-/-}$ mice; 129 × C57BL/6) mice were kindly provided by H. Bluethmann (Roche Center for Medical Genomics, Basel, Switzerland) (25). Germfree mice (BALB/c Yit) were kindly provided by H. Funabashi (Yakult Central Institute for Microbiological Research, Japan).

Fusion proteins and treatment protocol

Proteins comprised of the extracellular domain of either murine TNFR55 or LTβR fused to the hinge, C_H2, and C_H3 domains of human IgG1 (LTβR-Ig, TNFR55-Ig, and LFA-3-Ig, respectively) were used in our studies, as described elsewhere (19, 26, 27). Timed pregnant mice were injected i.v. with 200 μg of LTβR-Ig and/or 200 μg of TNFR55-Ig on gestational days 14 and 17, as described previously (5, 19). In some experiments, progeny of mice treated i.v. with LTβR-Ig and TNFR55-Ig on gestational period were further injected i.p. with 20 μg of LTβR-Ig, TNFR55-Ig, or human IgG1 (control) at weekly intervals from 7 days after birth and 50 μg of each Ig fusion protein from 4 wk old until age of 6 wk.

Cell purification

The mononuclear cells from CP and ILF of the large intestine were obtained with modified method, as described previously (8). In brief, the large intestine was opened longitudinally along the mesenteric wall, and mucus and feces were vigorously washed in the RPMI 1640 medium and wiped with filter paper. Subsequently, a section of intestine ~30 mm long was pasted on a plastic culture dish. The structures of CP and ILF are both circular in appearance, but the CP are larger than triple diameter of the ILF. Morphologically, the center of CP forms protruding configuration, and thus CP appears as dome-shaped tissue under a transillumination seromicroscope (Olympus TH3). In contrast, the ILF are recognized as flat shape. Blind test was conducted to count the number of ILF by three independent investigators by a transillumination seromicroscope. Then CP were taken with two sharp forceps and isolated, and a tiny fragment of ILF was isolated using a sharp needle (23 gauge; inner diameter, μm). CP and ILF were separately digested with collagenase (type IV, 0.5 mg/ml in RPMI 1640 including 2% FBS; Sigma-Aldrich) for 20 min in a 37°C incubator. This step was repeated until the architecture of tissue was totally disrupted. The single cell suspensions were pooled, washed, and placed on a discontinuous 40 and 70% Percoll gradient (Pharmacia). After centrifugation for 20 min at 600 × *g*, the cells were collected from the interface (8). To isolate the LP lymphocytes from the large intestine, mononuclear cells were dissociated using the collagenase digestion method after removal of CP and ILF, as described previously (28).

Flow cytometric analysis

A single lymphoid cell suspension was incubated with anti-FcγRII/III mAb (BD Pharmingen) and stained with FITC- or PE-conjugated anti-B220, CD3, IgD, IgM, or IgA mAbs (BD Pharmingen). The other aliquots of cells were incubated with each isotype control mAb, including rat IgG2b or rat IgG2a (BD Pharmingen). The profiles were analyzed using FACScan with CellQuest software (BD Biosciences). Reactivity with peanut agglutinin (PNA) was demonstrated using biotinylated PNA (Vector Laboratories), followed by streptavidin-PE.

Histochemical analysis

For the H&E staining, the large intestine was fixed in 4% paraformaldehyde and embedded in paraffin. The tissues were cut into 5-μm sections and stained with H&E (28). The sections were mounted and viewed under ×20 optics using a digital light microscope. Each of the images was analyzed with Photoshop (Adobe Systems). For the immunohistochemical study, freshly obtained large intestine was rapidly frozen in OCT embedding medium (Tissue-Tek) and stored at −80°C until processing (28). Cryostat sections (5 μm) were fixed in ice-cold acetone for 10 min, dried, and preblocked with anti-FcγRII/III mAb (BD Pharmingen) in PBS. Cells were stained with FITC-conjugated anti-CD11c mAb (BD Pharmingen) and PE-conjugated anti-B220 or CD3 mAbs (BD Pharmingen). The other aliquots of cells were incubated with each isotype control mAb, including hamster IgG, rat IgG2b, or rat IgG2a (BD Pharmingen). IgA-containing cells were visualized by FITC-conjugated anti-IgA mAb (BD Pharmingen). The sections were mounted and viewed under a dual red/green filter by confocal microscopy (Bio-Rad). Each of the images was analyzed with Photoshop (Adobe Systems) in a consistent manner, followed by overlying of the green and red images in the screen mode.

Scanning electron microscope analysis

For scanning electron microscopy analysis, large intestinal fragments of the double Ig-treated mice were cleaned of mucus and fixed in 2% glutaraldehyde and 2% paraformaldehyde in PBS containing 100 mM HEPES for 1 h at room temperature. After being washed with PBS, specimens were treated with 1% osmium tetroxide for 1 h at room temperature and then dehydrated in graded ethanol solution. Dehydrated tissues were critical point dried with CO_2, and sputter coated and observed with a scanning electron microscope (Hitachi).

Treatment with antibiotic water

For the antibiotic treatment, each group of 6-wk-old progenies was given antibiotics in drinking water for a period of 4 wk. The antibiotic water contained 500 mg/L ampicillin, 1 g/L neomycin sulfate, and 2 g/L of streptomycin (29).

RT-PCR

A standard quantitative RT-PCR protocol was used for the study for GAPDH-based quantitative RT-PCR (30). Total RNA was extracted from mononuclear cells isolated from LP of the large intestine or CP of naive mice or ILF of double Ig-treated mice by using the RNeasy mini kit (Qiagen), according to the manufacturer's protocol. A total of 1 μg of total RNA was reverse transcribed into cDNA using *Taq* Man reverse transcription kit (Applied Biosystems). Activation-induced cytidine deaminase (AID) mRNA levels were measured by real-time quantitative PCR method performed on the ABI PRISM 7500 (Applied Biosystems). For each treatment, two distinct amplifications were conducted in parallel to amplify

AID cDNA and GAPDH cDNA. The amplification reactions were performed in 25 μl vol containing 100 ng of cDNA per treatment, 12.5 μl of 2× TaqMan Universal PCR Master Mix (Applied Biosystems), and 1.25 μl of 20× Assays-on-Demand Gene Expression probe for AID (Applied Biosystems) or TaqMan GAPDH probe (Applied Biosystems). AID mRNA levels from each treatment were normalized to the corresponding amount of GAPDH mRNA levels. Water controls and samples without PCR mixtures were set up to eliminate the possibility of significant DNA contamination.

ELISPOT assay for total IgA Ab-forming cells

An ELISPOT assay was adopted to detect total numbers of IgA Ab-forming cells in the large intestine, as described previously (31).

Statistics

The data are expressed as the mean ± SE and compared using *t* test in Microsoft Excel Program.

Results

In utero blockade of LTβR- and TNFR-mediated signals induces the accelerated formation of ILF in the large intestine of mice

Using LTβR- and TNFR55-Ig fusion proteins as soluble antagonists, we tested whether LTαβ- and TNF-mediated signals influenced the formation of organized lymphoid tissues in the large intestine. For this purpose, mice were treated with TNFR55-Ig or LTβR-Ig or LTβR-Ig plus TNFR55-Ig (double Ig) fusion protein at gestational days 14 and 17. The exposure to LTβR-Ig or double Ig during the gestation period disrupted CP formation in the progeny, which confirmed our previous finding (23). Unexpectedly, however, careful light microscopy and H&E staining analysis revealed that numerous ILF existed throughout the mucosa of the large intestine of 6-wk-old mice treated in utero with LTβR-Ig or with double Ig fusion proteins (Fig. 1*A*). These changes in ILF development were not seen in the small intestine of these treated mice (6 wk old), but were unique to the large intestine. Interestingly, the progeny of mice treated with double Ig fusion protein in utero possessed more numerous ILF of larger size in the large intestine than those treated with LTβR-Ig alone. When the total number of ILF in the whole large intestine was counted under light microscopy, ~250 ILF were found in the progeny of mice treated with double Ig during gestation (Fig. 1*B*). In contrast, the numbers of ILF in control Ig-treated mice were 50 per large intestine (Fig. 1*B*). When mice were treated with TNFR55-Ig alone, no significant changes were seen in the total number of ILF in the large intestine. In all mice, ILF were preferentially located in the distal region of the large intestine (data not shown). An average of total recovered cell numbers of ILF isolated from the large intestine of the progeny of mice treated with double Ig fusion protein was 10-fold higher than control Ig-treated mice (3.0×10^6 vs 0.3×10^6) and 3-fold higher than LTβR-Ig-treated mice (3.0×10^6 vs 1.0×10^6). These observations suggest that ILF formation in the large intestine was accelerated by blockage of prenatal LTβR-mediated signals, and their maturation was further enhanced by the coblockage of TNFR-mediated signals during the selected gestational period.

Postnatal blockade of LTβR-mediated signals inhibits the accelerated formation of ILF in the large intestine of mice

To establish an exact role of TNFR and LTβR signaling after birth on the accelerated formation of ILF in the large intestine, the

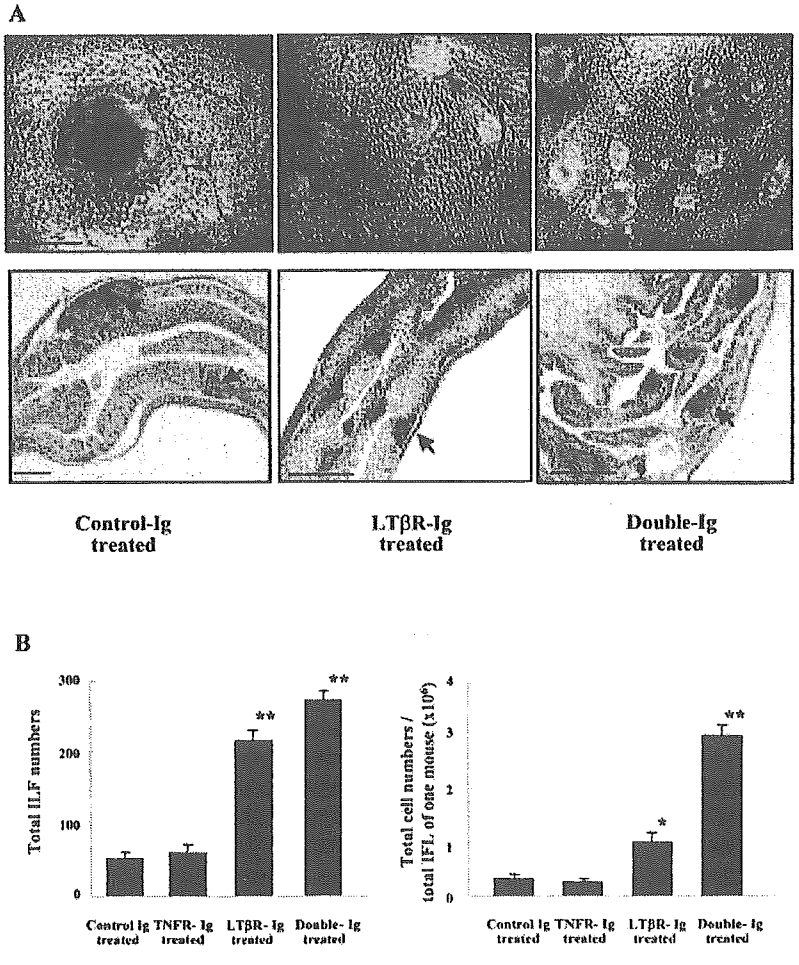

FIGURE 1. Effects of prenatal blockage of LT/LTβR and TNF/TNFR55 signal on the formation of ILF in the large intestine. Timed pregnant BALB/c mice were injected i.v. with TNFR55-Ig or LTβR-Ig and/or TNFR55-Ig (double IgG1) on gestational days 14 and 17. Purified human Ig was used as control Ig. *A*, Morphology of colonic patch (red arrow) and ILF (blue arrow) in the large intestine of each 6-wk-old progeny. The large intestine was opened longitudinally along the mesenteric wall, and a ~30-mm-long length of intestine was pasted onto the plastic culture dish. The picture was taken under the stereomicroscopy (*upper*). For the H&E staining, the large intestine was fixed in 4% paraformaldehyde and embedded in paraffin. The sections were viewed under ×20 optics with a digital light microscope (*below*). The bar indicates 50 μm. *B*, Total number of ILF in a whole large intestine was counted under a light microscope (*left*). Each ILF was then taken off with a sharp needle, and mononuclear cells were isolated and counted (*right*). The results are expressed as the mean ± SE from three mice per group and from a total of three experiments. *, $p < 0.05$, and **, $p < 0.01$ when compared with the number of ILF in the large intestine of control Ig-treated mice.

progenies of double Ig-treated mice on gestational period were further injected i.p. with LTβR-Ig or TNFR55-Ig or control Ig at weekly intervals from 1 wk after birth to age of 6 wk. Although the numbers of ILF were slightly lower, no significant difference was detected on the numbers of ILF in the large intestine of TNFR55-Ig-treated progenies compared with the control Ig-treated one. Interestingly, however, the large intestine of progenies postnatal treated with LTβR-Ig did not possess any ILF (Fig. 2). Furthermore, we have assessed the presence of ILF in the large intestine of TNF/LTα double-knockout mice that lack signaling pathways through both TNFR55 and LTβR. Interestingly, there are no ILF in the large intestine of those mice (Fig. 2). These findings indicate that the tissue genesis signaling pathway through LTβR, but not TNFR55, is required for the formation of ILF in the large intestine.

ILF in the large intestine contain B220$^+$, CD11c$^+$, and CD3$^+$ cells

To clarify the cell population in ILF of the large intestine, flow cytometric and immunohistochemical analyses were conducted using 6-wk-old progeny of mice treated in utero with control Ig or double Ig. Similar to the ILF in the small intestine (8, 20), immunohistochemical study revealed that LI-ILF were enriched with B cells (B220$^+$), with a limited frequency of dendritic stromal cells (CD11c$^+$) and T cells (CD3$^+$) (Fig. 3). Their cell population is phenotypically similar to the CP, but LI-ILF possesses more B220$^+$ cells and less CD3$^+$ cells than CP (Fig. 3). A major population of B220$^+$ cells in LI-ILF belongs to the IgD$^+$ and IgM$^+$ cells with some B220$^+$IgA$^-$ cells (Fig. 3). Similar to the phenotype of CP, LI-ILF possess detectable levels of B220$^+$IgA$^+$ cells, implying a role of LI-ILF as an inductive site for mucosal IgA responses. Interestingly, LI-ILF of mice treated with double Ig fusion protein in utero showed a higher density of CD3$^+$ cells when compared with those of control Ig-treated progeny (Fig. 3). Although the frequency of CD3$^+$ cells is increased in the treated LI-ILF, the follicle is still considered a B cell-enriched tissue because the frequency of B220$^+$ cells outnumbers CD3$^+$ cells (Fig. 3). In addition, flow cytometry analysis showed that LI-ILF of control Ig-treated progeny contained low numbers of germinal center-forming PNA$^+$ B cells; however, blockage of LTβR and TNFR55 signals during gestation enhanced the formation of germinal center-forming PNA$^+$ B cells (Fig. 3). These findings suggest that LI-ILF, similar to ILF in the small intestine, is one of key

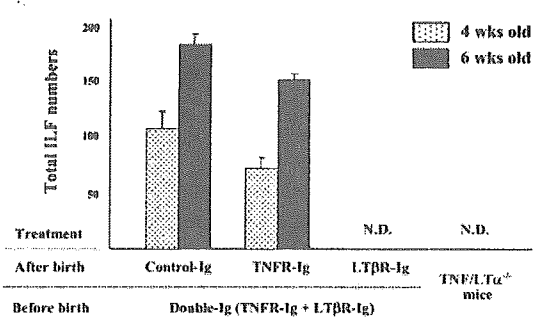

FIGURE 2. Effects of postnatal blockage of LT/LTβR or TNF/TNFR55 signal on the formation of ILF in the large intestine of the progenies treated in utero with the LTβR-Ig and TNFR55-Ig (double Ig). Progeny of mice treated i.v. with double Ig on gestational days 14 and 17 were further injected i.p. with 20 μg of LTβR-Ig or TNFR55-Ig or control Ig at weekly intervals from 7 days after birth and 50 μg of each Ig fusion protein from 4 wk old. Total numbers of ILF in a whole large intestine were counted under the stereomicroscope. The results are expressed as the mean ± SE from three mice per group and from a total of two experiments. N.D., not detectable.

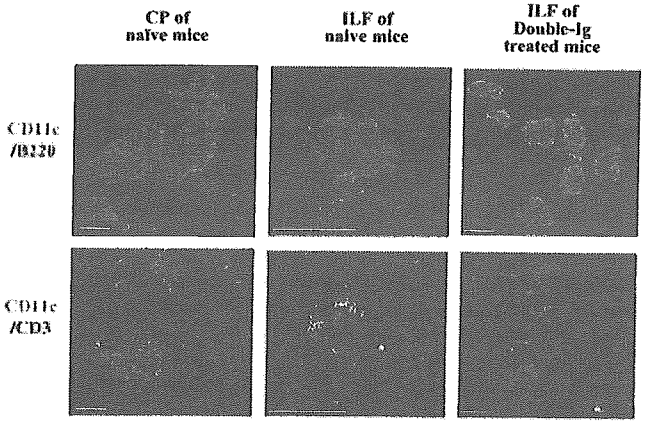

Mononuclear Cells	CP	ILF	
	Control-Ig	Control-Ig	Double-Ig
B220$^+$	77.4± 2.5	86.9± 3.4	86.2± 3.9
CD3$^+$	13.3± 1.2	5.7± 0.5	10.0± 2.2
IgD$^+$ / IgM$^+$	57.5± 3.8	32.0± 1.8	44.8± 2.2
PNA$^+$ / B220$^+$	5.4± 1.1	1.0± 0.2	6.4± 1.0
B220$^+$ / IgA$^+$	10.5± 1.2	5.6± 1.0	6.3± 0.2

FIGURE 3. Characterization of mononuclear cells in the LI-ILF and CP of mice in utero treated with LTβR-Ig and TNFR55-Ig fusion proteins, as described in Fig. 1 legend. Immunofluorescence staining (*upper picture*) and FACS analysis of mononuclear cells isolated from CP and ILF of the large intestine (table). For the immunohistochemical study, the large intestine of 6-wk-old progenies was rapidly frozen, and cryostat sections were stained with FITC-conjugated anti-CD11c mAb and PE-conjugated anti-B220 mAb or PE-conjugated anti-CD3 mAb. The FACS results are expressed as the mean ± SE from three mice per group and from a total of two experiments. The bar indicates 50 μm.

mucosal inductive tissues for initiation of IgA responses. Furthermore, LTβR- and TNFR55-mediated signal play a critical role in the control of LI-ILF development.

Chronological analysis of escalated LI-ILF formation in double Ig-treated mice

Because we found large numbers of ILF in the large intestine of 6-wk-old progeny following the gestational blockage of LTβR- and TNFR55-mediated signals, we further examined the effect of double Ig treatment on kinetics of their development. For this purpose, we compared ILF number in the small and large intestine of progeny of mice treated with control Ig or double Ig at age of 3, 10, and 24 wk. When the control Ig-treated mice were examined, the numbers of ILF in both small and large intestine were gradually increased (Fig. 4). Interestingly, maximum numbers of LI-ILF were already reached as early as 3 wk old among progeny of mice treated with double Ig (Fig. 4). The total numbers of ILF were then maintained up to 24 wk old. In contrast, ILF in the small intestine of progeny treated with control Ig or double Ig fusion protein gradually developed and reached the maximum numbers at the age of 24 wk old. It was also noted that total numbers of small intestinal ILF were higher in mice treated with the double Ig in utero when compared with the control Ig-treated mice. The fact that the accelerated ILF formation in the large intestine by gestational blockage of LTβR and TNFR55 signals occurred very early after birth implied that their formation and development might not be influenced by exogenous environmental factors, such as gut microflora.

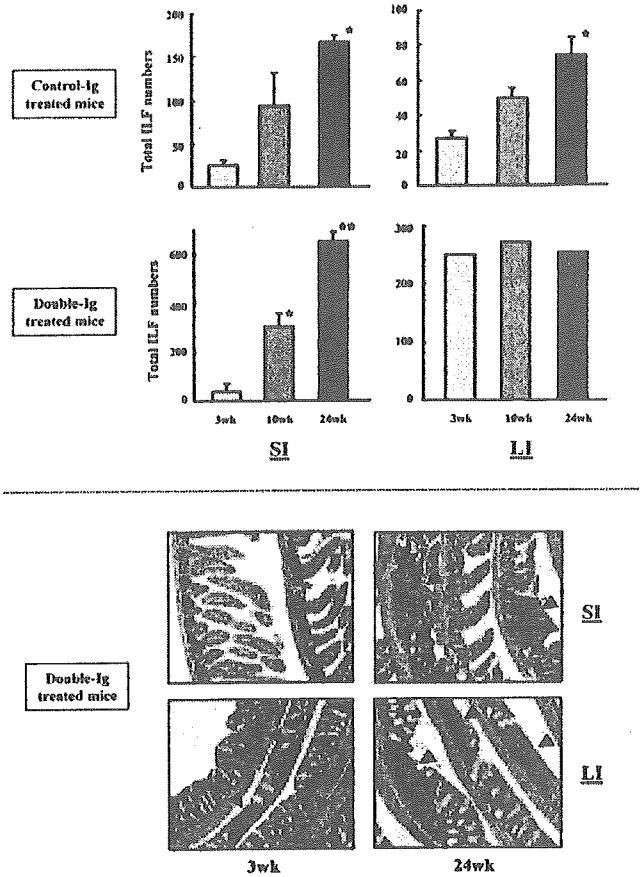

FIGURE 4. Chronological influences on the increased LI-ILF development in mice in utero treated with LTβR-Ig and TNFR55-Ig (double Ig). Numbers of ILF in the small and large intestines (SI and LI, respectively) of mice treated in utero with control Ig or double Ig fusion protein under the stereomicroscopy, as described in Fig. 1 legend. For the H&E staining, the sections were viewed under ×20 optics with a digital light microscope. The progenies were sacrificed, and the total number of ILF in a whole small and large intestine at 3, 10, and 24 wk old was counted. The results are expressed the mean ± SE from three mice per group and from a total of two experiments. *, $p < 0.05$, and **, $p < 0.01$ when compared with the number of ILF of the 3-wk-old progeny.

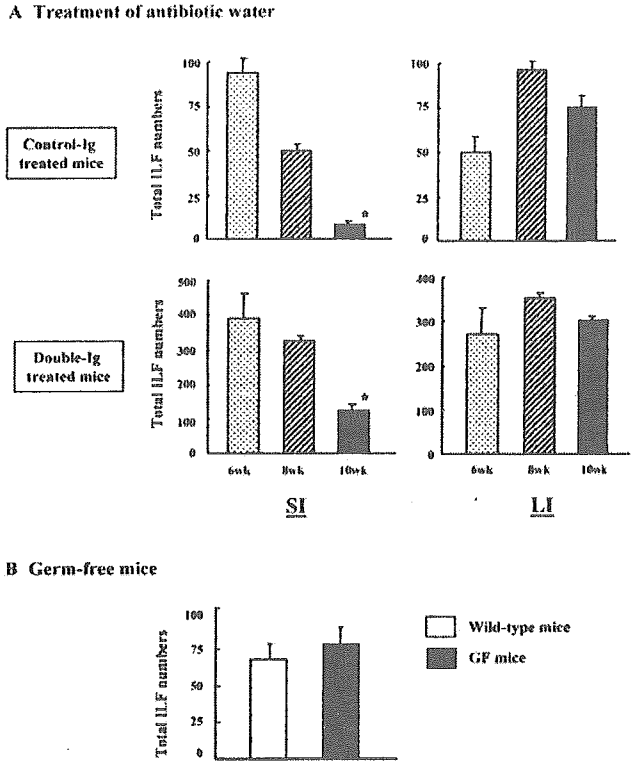

FIGURE 5. Effects of gut microflora on the formation and development of ILF in the small and large intestine. *A*, Both groups of 6-wk-old mice treated with control or LTβR-Ig and TNFR55-Ig (double Ig) fusion protein in utero were fed for 4 wk with antibiotic water containing ampicillin, neomycin sulfate, and streptomycin. At 2 wk (8 wk old) or 4 wk (10 wk old) after antibiotic treatment, the total number of ILF in a whole small and large intestine was counted under light microscope, as described in the Fig. 1 legend. *B*, The total number of ILF in the large intestine of germfree mice was counted. The results are expressed as the mean ± SE from three mice per group and from a total of three experiments. *, $p < 0.05$ when compared with non-antibiotic-treated mice.

The development of LI-ILF is independent from influences of gut microflora

Several previous studies have demonstrated a critical role of gut microflora on the ILF formation in the small intestine (8, 20, 29). To determine the potential involvement of intestinal microflora on the ILF hyperplasia in the large intestine following the prenatal blockage of LTβR and TNFR55 signals, we altered the microflora by oral administration of antibiotic water, which reduced both aerobic and anaerobic bacteria (29). Both groups of 6-wk-old progenies were fed antibiotic water for 4 wk and sacrificed at 2 and 4 wk after feeding. To see the effectiveness of the antibiotic treatment, the bacteria load was determined in the feces of control Ig- and double Ig-treated mice before and after antibiotic treatment. Essentially, no bacteria were remaining after the feeding of antibiotic water (data not shown). As shown in Fig. 5*A*, the antibiotic water treatment drastically decreased ILF formation in the small intestine in both groups of mice treated in utero with control Ig or double Ig. However, strikingly, LI-ILF formation in the double Ig-treated progeny was not influenced by the antibiotic treatment, and maximum numbers of LI-ILF were not changed even after prolonged antibiotic water treatment (Fig. 5*A*). Furthermore, the numbers of LI-ILF were comparable in the germfree mice to those of wild-type mice (Fig. 5*B*). These results indicate that development of ILF in the large intestine is not influenced by the gut bacterial flora.

LI-ILF possess M cells on the FAE region and express AID mRNA

To determine whether LI-ILF possess the ability of Ag uptake from the lumen of intestine, we examined the presence of M cells on the FAE of LI-ILF from the double Ig-treated mice. As indicated in Fig. 6*A*, LI-ILF revealed a hallmark feature of M cells, i.e., a depressed surface with short and irregular microvilli. These results suggest that LI-ILF might play as Ag sampling site as like as the other organized mucosa-associated lymphoid tissues, e.g., colonic patches.

To assess the ability of IgA class switching in the LI-ILF, the expression levels of AID mRNA, which plays an essential role in class switching recombination and somatic hypermutation of Ig genes, were determined (32). The mononuclear cells isolated from LI-ILF of mice treated with double Ig in utero expressed AID mRNA (Fig. 6*B*). In contrast to ILF, AID mRNA was not detectable in the diffused LP region of the large intestine (Fig. 6*B*). These findings suggest that the levels of μ to α class switching are increased in the large intestine of mice treated with double Ig in utero due to the maximum increase of ILF numbers. Thus, one can

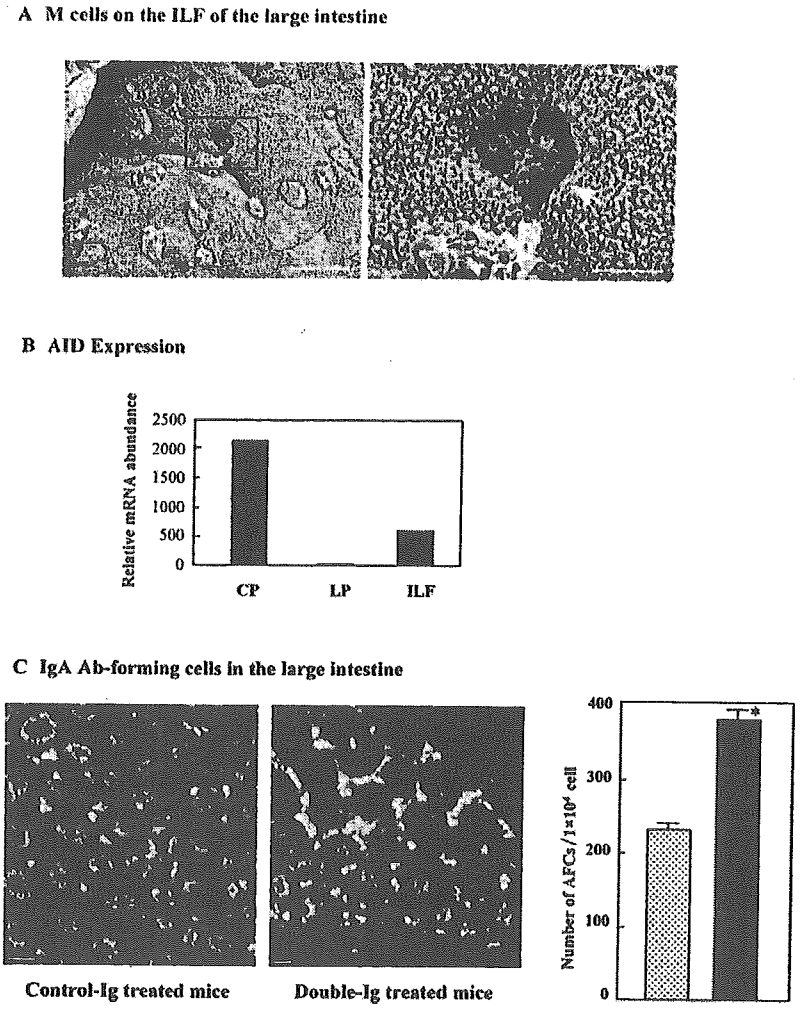

FIGURE 6. *A*, The presence of M cells on the FAE of LI-ILF of mice prenatally treated with LTβR-Ig and TNFR55-Ig (double Ig) fusion protein. *B* and *C*, The mRNA expression of AID and the number of IgA Ab-secreting cells in the large intestine of mice treated with control Ig or double Ig fusion protein in utero. A quantitative RT-PCR was performed using mononuclear cells isolated from LP in the large intestine of control Ig-treated mice and from ILF in the large intestine of double Ig-treated mice. As positive control for a quantitative RT-PCR, CP of control Ig-treated mice were adopted. For the immunohistochemical study (*C*, *left*), the large intestine of 6-wk-old progenies of both groups were rapidly frozen, and cryostat sections were stained with FITC-conjugated anti-IgA. ELISPOT assay was adopted to further confirm the number of IgA Ab-forming cells in the LP of the large intestine of mice treated with control Ig (▨) or double Ig (■) fusion protein in utero (*C*, *right*). The results are expressed as the mean ± SE from five mice per group and from a total of two experiments. The bar indicates 10 μm (*A*, *left*) and 2.5 μm (*A*, *right*).

predict the subsequent elevation of IgA-producing cells in the large intestine of these mice. The numbers of IgA-producing cells were therefore assessed, using the large intestine of the 6-wk-old mice treated in utero with control Ig or double Ig. Interestingly, increased numbers of IgA-expressing cells were detected in the LP region of the large intestine of in utero double Ig-treated mice when compared with the control mice (Fig. 6*C*, *left*). The results were also confirmed by the analysis of single cells using ELISPOT assay. The numbers of IgA-producing cells were increased in mononuclear cells isolated from the large intestine of mice treated with double Ig in utero when compared with the control Ig-treated mice (Fig. 6*C*, *right*). These results further support a notion that ILF may play a role for induction of IgA^+ B cells in the large intestine.

Discussion

In general, a family of inflammatory cytokine-mediated signals provided via LTβR and TNFR55 is considered to be critical for the organogenesis of secondary lymphoid tissue (18, 33). One can consider the organogenic steps that take place during development as a form of programmed inflammation, given what we now know about the steps underlying the genesis of tertiary lymphoid structures in chronic disease settings (34). In this study, we demonstrated that prenatal blockage of LT/LTβR signaling cascade resulted in the acceleration of ILF formation in the large intestine, and further that prenatal blockage of TNF/TNFR55 signal enhanced their maturation. The hyperplasia of LI-ILF was not due to stimulation of exogenous environmental stimuli, such as microflora Ags. Most interestingly, LI-ILF expressed AID mRNA, and therefore might be critically involved in the generation of IgA-committed B cells. Thus, our present study is the first one to show the unique characteristics of LI-ILF as IgA-inductive sites, whose development is accelerated by the blockage of LTβR and TNFR55 in utero.

Normal numbers of ILF were present in the small intestine of mice treated with LTβR-Ig fusion protein in utero, but were absent in the $LT\alpha^{-/-}$ mice and $aly/aly^{-/-}$ mice, suggesting that ILF formation in the small intestine did not require gestational LT/LTβR-dependent event, but needed the postnatal signals (8). In addition, a recent study demonstrated that, unlike PP, postnatal LT/LTβR signals are required for ILF formation in the small intestine, and additional TNF/TNFR55 signal and exogenous stimuli were needed for their maturation (20). In contrast, limited information is currently available on the immunological function and tissue genesis of ILF (or solitary lymphoid aggregates) in the large intestine. For example, in utero treatment with LTβR-Ig ablated the formation of CP, but scattered B cell aggregates in the mucosal layer of large intestine were retained (23). Furthermore, the progeny of mice treated with LTβR-Ig plus TNFR55-Ig fusion protein were reported to have some submucosal lymphoid patches in the large intestine (24). In the present study, we demonstrate that prenatal blockage of LT/LTβR signal enhanced the formation of LI-ILF,

and prenatal blockage of LT/LTβR plus TNF/TNFR signals further accelerated this phenomenon and resulted in extreme hyperplasia of LI-ILF. It is clear that LI-ILF used LT/LTβR and TNF/TNFR signals in a different manner than other gut-associated lymphoid tissues such as PP and CP. An interesting possibility is that LTβR- and TNFR-mediated signaling might behave as a negative regulation for the LI-ILF genesis in the gestational period.

Several recent studies demonstrated a critical involvement of gut flora on the development of ILF in the small intestine. It has been reported that normal numbers of ILF were detected in the small intestine of germfree mice (8). However, another study showed that the development of ILF in the small intestine did not occur in germfree mice, but, if germfree mice were conventionalized, modest number of mature ILF developed (20). Further augmentation of ILF formation in the small intestine was induced by in utero treatment with LTβR-Ig fusion protein (20). Fagarasan et al. (29) recently revealed that alteration of bacteria flora by antibiotic treatment abolished ILF hyperplasia and germinal center enlargement in the small intestine that was provoked by the genetic deficiency of AID. Furthermore, the number of anaerobic bacteria was 100-fold increased in the small intestines of $AID^{-/-}$ mice than $AID^{+/-}$; however, no significant changes were detected in the large intestine of $AID^{-/-}$ mice (29). Those results are consistent with our present results showing that the total number of ILF in the small intestine of naive mice and mice treated with double Ig in utero was significantly reduced by antibiotic treatment. However, the formation of LI-ILF of both naive and the double Ig-treated mice was not influenced by the antibiotic treatment. The fact that extreme hyperplasia of ILF in the large intestine of double Ig-treated mice was not due to stimulation of gut microflora suggests that bacterial Ag may not be involved in the development and maturation of LI-ILF. Hence, although the immunological nature of ILF in the small and large intestine seems identical in terms of cell populations and morphologic features, regulatory factors associated with programmed inflammation for their tissue genesis and maturation might be significantly different due to the different exogenous environments. We are investigating the exact regulatory factors that are specifically involved in the development of LI-ILF. In particular, an understanding of the identification and ontogeny of the cells required to induce local LI-ILF formation will be critical, as it appears these cells require LTβR and TNFR signals during embryogenesis that regulate their activity. Furthermore, the identity and regulation of the specific molecules critical for induction of LI-ILF need further study, as it is likely that these are further involved in the regulation of colon-associated diseases.

We have also demonstrated that ILF are abundantly developed in the large intestine in the absence of CP. These plentiful ILF that developed in CP-null large intestine could be a key site for the continuous generation of IgA-committed B cells. Interestingly, our present study showed mononuclear cells isolated from CP and ILF of normal mice, but not from intestinal LP, expressed high levels of AID mRNA that play an essential role for isotype switching recombination and somatic hypermutation of Ig. Furthermore, enhanced numbers of IgA-producing cells were noted in the LP region of large intestine of progenies with numerous numbers of ILF, but no CP by the gestational blockage of LT/LTβR and TNF/TNFR55 signaling pathways. Based upon their cell phenotype and micro- and macromorphology, it is reasonable to classify LI-ILF as an inductive site for intestinal IgA production in addition to CP. Therefore, LI-ILF and CP may form a reciprocal inductive network in mucosal immunity. Thus, the increased IgA response seen in the CP-null mice could be explained as a compensatory response in the absence of CP. Taken together, both ILF and CP in the large intestine are integrated inductive tissues that can compensate each other for the induction of mucosal IgA responses.

A possible contribution of LI-ILF to the development of colon-restricted inflammatory disease is just beginning to be understood. A previous study described that elimination of PP and CP, but not scattered aggregates of B cells by in utero treatment with LTβR-Ig fusion protein, resulted in the prevention of trinitrobenzenesulfonic acid-induced Th2 cell type colitis development (23). In contrast, another group found a more severe type of dextran sodium sulfate-induced colitis in PP- and mesenteric lymph node-null mice generated by the in utero treatment with LTβR-Ig and TNFR55-Ig fusion proteins (24). Although these mice did not possess peripheral lymphoid tissue, they found that there were submucosally located lymphoid follicles in the large intestine consisting of B and T cell areas. Furthermore, dextran sodium sulfate-induced colitis accelerated additional formation of these lymphoid follicles (24). In all cases of ulcerative colitis patients, the colonic LP contain numerous basal lymphoid aggregates composed of T and B lymphocytes and dendritic cells (35). Furthermore, these lymphoid aggregates increase in number and size with severity of disease (35). Overall, it seems likely that LI-ILF could be site for the generation of regulatory and/or pathogenic lymphocytes. Thus, both in human patients and in mouse disease models, LI-ILF hyperplasia is associated with colonic disease. Furthermore, whether ILF induces regulatory type responses or pathogenic type responses may depend on surrounding environmental and immunological conditions. To further address these questions, our murine model of LI-ILF hyperplasia will be useful to clarify their precise role in the control of large intestine-restricted diseases.

Disclosures

The authors have no financial conflict of interest.

References

1. Kiyono, H., J. Bienenstock, J. R. McGhee, and P. B. Ernst. 1992. The mucosal immune system: features of inductive and effector sites to consider in mucosal immunization and vaccine development. *Reg. Immunol. 4:54.*
2. McGhee, J. R., and H. Kiyono. 1999. The mucosal immune system. In *Fundamental Immunology*, 4th Ed. W. E. Paul, ed. Lippincott-Raven Publishers, New York, p. 909.
3. Keren, D. F., P. S. Holt, H. H. Collins, P. Gemski, and S. B. Formal. 1978. The role of Peyer's patches in the local immune response of rabbit ileum to live bacteria. *J. Immunol. 120:1892.*
4. Craig, S. W., and J. J. Cebra. 1971. Peyer's patches: an enriched source of precursors for IgA-producing immunocytes in the rabbit. *J. Exp. Med. 134:188.*
5. Yamamoto, M., P. Rennert, J. R. McGhee, M. N. Kweon, S. Yamamoto, T. Dohi, S. Otake, H. Bluethmann, K. Fujihashi, and H. Kiyono. 2000. Alternate mucosal immune system: organized Peyer's patches are not required for IgA responses in the gastrointestinal tract. *J. Immunol. 164:5184.*
6. Kang, H. S., R. K. Chin, Y. Wang, P. Yu, J. Wang, K. A. Newell, and Y. X. Fu. 2002. Signaling via LTβR on the lamina propria stromal cells of the gut is required for IgA production. *Nat. Immunol. 3:576.*
7. Fagarasan, S., K. Kinoshita, M. Muramatsu, K. Ikuta, and T. Honjo. 2001. In situ class switching and differentiation to IgA-producing cells in the gut lamina propria. *Nature 413:639.*
8. Hamada, H., T. Hiroi, Y. Nishiyama, H. Takahashi, Y. Masunaga, S. Hachimura, S. Kaminogawa, H. Takahashi-Iwanaga, T. Iwanaga, H. Kiyono, et al. 2002. Identification of multiple isolated lymphoid follicles on the antimesenteric wall of the mouse small intestine. *J. Immunol. 168:57.*
9. Smith, C. A., T. Farrah, and R. G. Goodwin. 1994. The TNF receptor superfamily of cellular and viral proteins: activation, costimulation, and death. *Cell 76:959.*
10. Ware, C. F., T. L. VanArsdale, P. D. Crowe, and J. L. Browning. 1995. The ligands and receptors of the lymphotoxin system. *Curr. Top. Microbiol. Immunol. 198:175.*
11. Vandenabeele, P., W. Declercq, B. Vanhaesebroeck, J. Grooten, and W. Fiers. 1995. Both TNF receptors are required for TNF-mediated induction of apoptosis in PC60 cells. *J. Immunol. 154:2904.*
12. Gruss, H. J., and S. K. Dower. 1995. Tumor necrosis factor ligand superfamily: involvement in the pathology of malignant lymphomas. *Blood 85:3378.*
13. Browning, J. L., I. D. Sizing, P. Lawton, P. R. Bourdon, P. D. Rennert, G. R. Majeau, C. M. Ambrose, C. Hession, K. Miatkowski, D. A. Griffiths, et al. 1997. Characterization of lymphotoxin-αβ complexes on the surface of mouse lymphocytes. *J. Immunol. 159:3288.*
14. De Togni, P., J. Goellner, N. H. Ruddle, P. R. Streeter, A. Fick, S. Mariathasan, S. C. Smith, R. Carlson, L. P. Shornick, and J. Strauss-Schoenberger. 1994.

Abnormal development of peripheral lymphoid organs in mice deficient in lymphotoxin. *Science 264:703.*

15. Alimzhanov, M. B., D. V. Kuprash, M. H. Kosco-Vilbois, A. Luz, R. L. Turetskaya, A. Tarakhovsky, K. Rajewsky, S. A. Nedospasov, and K. Pfeffer. 1997. Abnormal development of secondary lymphoid tissues in lymphotoxin β-deficient mice. *Proc. Natl. Acad. Sci. USA 94:9302.*
16. Futterer, A., K. Mink, A. Luz, M. H. Kosco-Vilbois, and K. Pfeffer. 1998. The lymphotoxin β receptor controls organogenesis and affinity maturation in peripheral lymphoid tissues. *Immunity 9:59.*
17. Koni, P. A., R. Sacca, P. Lawton, J. L. Browning, N. H. Ruddle, and R. A. Flavell. 1997. Distinct roles in lymphoid organogenesis for lymphotoxins α and β revealed in lymphotoxin β-deficient mice. *Immunity 6:491.*
18. Rennert, P. D., J. L. Browning, and P. S. Hochman. 1997. Selective disruption of lymphotoxin ligands reveals a novel set of mucosal lymph nodes and unique effects on lymph node cellular organization. *Int. Immunol. 9:1627.*
19. Rennert, P. D., J. L. Browning, R. Mebius, F. Mackay, and P. S. Hochman. 1996. Surface lymphotoxin α/β complex is required for the development of peripheral lymphoid organs. *J. Exp. Med. 184:1999.*
20. Lorenz, R. G., D. D. Chaplin, K. G. McDonald, J. S. McDonough, and R. D. Newberry. 2003. Isolated lymphoid follicle formation is inducible and dependent upon lymphotoxin-sufficient B lymphocytes, lymphotoxin β receptor, and TNF receptor I function. *J. Immunol. 170:5475.*
21. Owen, R. L., A. J. Piazza, and T. H. Ermak. 1991. Ultrastructural and cytoarchitectural features of lymphoreticular organs in the colon and rectum of adult BALB/c mice. *Am. J. Anat. 190:10.*
22. Dohi, T., K. Fujihashi, P. D. Rennert, K. Iwatani, H. Kiyono, and J. R. McGhee. 1999. Hapten-induced colitis is associated with colonic patch hypertrophy and T helper cell 2-type responses. *J. Exp. Med. 189:1169.*
23. Dohi, T., P. D. Rennert, K. Fujihashi, H. Kiyono, Y. Shirai, Y. I. Kawamura, J. L. Browning, and J. R. McGhee. 2001. Elimination of colonic patches with lymphotoxin β receptor-Ig prevents Th2 cell-type colitis. *J. Immunol. 167:2781.*
24. Spahn, T. W., H. Herbst, P. D. Rennert, N. Lugering, C. Maaser, M. Kraft, A. Fontana, H. L. Weiner, W. Domschke, and T. Kucharzik. 2002. Induction of colitis in mice deficient of Peyer's patches and mesenteric lymph nodes is associated with increased disease severity and formation of colonic lymphoid patches. *Am. J. Pathol. 161:2273.*
25. Eugster, H. P., M. Muller, U. Karrer, B. D. Car, B. Schnyder, V. M. Eng, G. Woerly, M. Le Hir, F. di Padova, M. Aguet, et al. 1996. Multiple immune abnormalities in tumor necrosis factor and lymphotoxin-α double-deficient mice. *Int. Immunol. 8:23.*
26. Force, W. R., B. N. Walter, C. Hession, R. Tizard, C. A. Kozak, J. L. Browning, and C. F. Ware. 1995. Mouse lymphotoxin-β receptor: molecular genetics, ligand binding, and expression. *J. Immunol. 155:5280.*
27. Miller, G. T., P. S. Hochman, W. Meier, R. Tizard, S. A. Bixler, M. D. Rosa, and B. P. Wallner. 1993. Specific interaction of lymphocyte function-associated antigen 3 with CD2 can inhibit T cell responses. *J. Exp. Med. 178:211.*
28. Kweon, M. N., M. Yamamoto, M. Kajiki, I. Takahashi, and H. Kiyono. 2000. Systemically derived large intestinal $CD4^+$ Th2 cells play a central role in STAT6-mediated allergic diarrhea. *J. Clin. Invest. 106:199.*
29. Fagarasan, S., M. Muramatsu, K. Suzuki, H. Nagaoka, H. Hiai, and T. Honjo. 2002. Critical roles of activation-induced cytidine deaminase in the homeostasis of gut flora. *Science 298:1424.*
30. Bunda, S., N. Kaviani, and A. Hinek. 2005. Fluctuations of intracellular iron modulate elastin production. *J. Biol. Chem. 280:2341.*
31. Fujihashi, K., J. R. McGhee, M. N. Kweon, M. D. Cooper, S. Tonegawa, I. Takahashi, T. Hiroi, J. Mestecky, and H. Kiyono. 1996. γ/δ T cell-deficient mice have impaired mucosal immunoglobulin A responses. *J. Exp. Med. 183:1929.*
32. Muramatsu, M., K. Kinoshita, S. Fagarasan, S. Yamada, Y. Shinkai, and T. Honjo. 2000. Class switch recombination and hypermutation require activation-induced cytidine deaminase (AID), a potential RNA editing enzyme. *Cell 102:553.*
33. Rennert, P. D., D. James, F. Mackay, J. L. Browning, and P. S. Hochman. 1998. Lymph node genesis is induced by signaling through the lymphotoxin β receptor. *Immunity 9:71.*
34. Kratz, A., A. Campos-Neto, M. Hanson, and N. Ruddle. 1996. Chronic inflammation caused by lymphotoxin is lymphoid neogenesis. *J. Exp. Med. 183:1461.*
35. Yeung, M. M., S. Melgar, V. Baranov, A. Oberg, A. Danielsson, S. Hammarstrom, and M. L. Hammarstrom. 2000. Characterization of mucosal lymphoid aggregates in ulcerative colitis: immune cell phenotype and TcR-γδ expression. *Gut 47:215.*

GASTROENTEROLOGY 2005;128:922–934

Colitis in Mice Lacking the Common Cytokine Receptor γ Chain Is Mediated by IL-6–Producing CD4+ T Cells

YASUYUKI KAI,*,† ICHIRO TAKAHASHI,*,§ HIROMICHI ISHIKAWA,¶ TAKACHIKA HIROI,*,‖ TSUNEKAZU MIZUSHIMA,† CHU MATSUDA,† DAISUKE KISHI,*† HIROMASA HAMADA,¶ HIROSHI TAMAGAWA,*,† TOSHINORI ITO,† KAZUYUKI YOSHIZAKI,# TADAMITSU KISHIMOTO,** HIKARU MATSUDA,† and HIROSHI KIYONO*,‖

*Department of Mucosal Immunology, Research Institute for Microbial Diseases, †Department of Surgery, Graduate School of Medicine, #Department of Medical Science, School of Health & Sport Science, and **Graduate School of Frontier Biosciences, Osaka University, Osaka; §Department of Mucosal Immunology, Graduate School of Biomedical Science, Hiroshima University, Hiroshima; ¶Department of Microbiology, Keio University School of Medicine, Tokyo; and ‖Division of Mucosal Immunology, Department of Microbiology and Immunology, The Institute of Medical Science, The University of Tokyo, Tokyo, Japan

Background & Aims: **Mice that have a truncated mutation of the common cytokine receptor γ chain (CRγ$^{-/Y}$) are known to spontaneously develop colitis. To identify the pathologic elements responsible for triggering this localized inflammatory disease, we elucidated and characterized aberrant T cells and their enteropathogenic cytokines in CRγ$^{-/Y}$ mice with colitis.** *Methods:* **The histologic appearance, cell population, T-cell receptor Vβ usage, and cytokine production of lamina propria lymphocytes were assessed. CRγ$^{-/Y}$ mice were treated with anti-interleukin (IL)-6 receptor monoclonal antibody to evaluate its ability to control colitis, and splenic CD4+ T cells from the same mouse model were adoptively transferred into SCID mice to see if they spurred the appearance of colitis.** *Results:* **We found marked thickening of the large intestine, an increase in crypt depth, and infiltration of the colonic lamina propria and submucosa with mononuclear cells in the euthymic CRγ$^{-/Y}$ mice, but not in the athymic CRγ$^{-/Y}$ mice, starting at the age of 8 weeks. Colonic CD4+ T cells with high expressions of antiapoptotic Bcl-x and Bcl-2 were found to use selected subsets (Vβ14) of T-cell receptor and to exclusively produce IL-6. Treatment of CRγ$^{-/Y}$ mice with anti–IL-6 receptor monoclonal antibody prevented the formation of colitis via the induction of apoptosis in IL-6–producing CD4+ T cells. Adoptive transfer of pathologic CD4+ T cells induced colitis in the recipient SCID mice.** *Conclusions:* **Colonic IL-6–producing thymus-derived CD4+ T cells are responsible for the development of colitis in CRγ$^{-/Y}$ mice.**

The gastrointestinal immune system is continuously exposed to a harsh environment of microbial and mitogenic stimulation. To maintain immunologic homeostasis, the gastrointestinal mucosa is equipped with a regulatory T-cell network formed by an array of subsets of αβ or γδ T-cell receptor (TCR)-bearing T cells (αβ or γδ T cells). A delicate balance between Th1- and Th2-type CD4+ αβ T cells is essential for the induction and regulation of a secretory immunoglobulin (Ig) A response.[1] Interferon (IFN)-γ, a well-known Th1 cell–derived cytokine, induces secretory component (or polymeric Ig receptor) production by epithelial cells for the formation and transport of secretory IgA.[2] IgA-enhancing cytokines such as interleukin (IL)-5 and IL-6, which are produced by Th2 cells, induce IgA-committed B cells to differentiate into IgA plasma cells.[1] Further, Th3 cells and/or regulatory T cells (Tr1 cells) produce transforming growth factor (TGF)-β and IL-10, 2 suppressor cytokines that prevent inflammation and induce oral tolerance.[3] γδ T cells have also been shown to be involved in the regulation of IgA responses.[4]

Immunologic diseases of the gastrointestinal tract, such as inflammatory bowel disease (IBD), may occur when the immunologic harmony of the regulatory T-cell network is disturbed, as by alterations of intestinal environments, including cytokines and their receptor-mediated signaling cascades, and the gut microflora.[5–10] Indeed, chronic IBD-like disease development has been observed in mice that have undergone various targeted disruptions of cytokine genes,[11,12] TCR components,[13–15] or a G-protein gene.[16] Further, most of these inflamma-

Abbreviations used in this paper: CRγ, common cytokine receptor γ chain; ELISA, enzyme-linked immunosorbent assay; FACS, fluorescence-activated cell sorter; FITC, fluorescein isothiocyanate; GAPDH, glyceraldehyde-3-phosphate dehydrogenase; IFN, interferon; IL, interleukin; IL-6R, interleukin-6 receptor; LCR, LightCycler Red 640; LP, lamina propria; mAb, monoclonal antibody; PCR, polymerase chain reaction; PE, phycoerythrin; SP, spleen; TCR, T-cell receptor; TGF, transforming growth factor; TNF, tumor necrosis factor.

0016-5085/05/$30.00
doi:10.1053/j.gastro.2005.01.013

tory diseases do not occur in the absence of gastrointestinal flora.[17–19]

The murine common cytokine receptor γ chain (CRγ) is a 64-kilodalton type-1 transmembrane protein of the cytokine receptor family.[20,21] CRγ alone is unable to bind to cytokines, but the γ chain is an essential component of the cell-surface receptor complexes of IL-2, IL-4, IL-7, IL-9, and IL-15.[20,22] Disruption of the CRγ has been shown to result in an absence or severe reduction in numbers of natural killer cells, decreased numbers of T cells (including thymus-independent T cells) and B cells, marked hypoplasia of the thymus and peripheral lymphoid tissues, defective formation of lymphoid follicles,[22,23] and marked splenomegaly and mesenteric lymphadenopathy.[24,25] Disruption of CRγ is also known to lead the gut-associated tissue and mucosal γδ T cells deficient in key elements, thereby disturbing the mucosal immune system,[22] and $CR\gamma^{-/Y}$ mice spontaneously develop chronic large intestinal inflammation. Thus, we decided to examine the possible pathologic elements responsible for the development of intestinal inflammation and the cellular and molecular aspects of the pathology seen in $CR\gamma^{-/Y}$ mice, focusing on aberrant T cells and their enteropathogenic cytokines.

Materials and Methods

Mice

Euthymic (nu/+) mutant $CR\gamma^{-/Y}$, euthymic (nu/+) wild-type $CR\gamma^{+/Y}$, and athymic (nu/nu) mutant $CR\gamma^{-/Y}$ mice (Japan Clea, Tokyo, Japan) were used for the generation of $CR\gamma^{-/Y}$ mutants with a BALB/c background. The original $CR\gamma^{-/x}$ mice with B6 background[26] were crossed with athymic BALB/c mice, and their heterozygous $CR\gamma^{-/x}$ progeny were backcrossed to athymic BALB/c mice to obtain euthymic (nu/+) wild-type $CR\gamma^{+/Y}$, euthymic (nu/+) mutant $CR\gamma^{-/Y}$, and athymic (nu/nu) mutant $CR\gamma^{-/Y}$ littermates. Male $CR\gamma^{-/Y}$ offspring were typed by polymerase chain reaction (PCR) analysis of tail DNA with a set of primers to the neomycin-resistant gene described elsewhere.[27] All mice used for experiments were between 6 and 20 weeks of age, and the absence of the thymus was checked at necropsy. $CR\gamma^{-/Y}$ mice on a BALB/c background were obtained from the B6 mice backcrossed more than 20 times to athymic BALB/c nude mice. The mice were housed in the Experimental Animal Facility at the Research Institute for Microbial Diseases at Osaka University. All mice were kept on a 12-hour light/dark cycle and received sterilized food and autoclaved distilled water ad libitum.

Isolation of Lymphoid Cells From Mucosa-Associated Tissues and Spleen

Spleen (SP) and mesenteric lymph nodes were aseptically removed, and single-cell suspensions were prepared by a standard mechanical disruption procedure.[4,14,15] Single-cell suspensions of Peyer's patches and lamina propria (LP) lymphocytes were prepared by an enzymatic dissociation method, using collagenase as previously described.[4,14,15] The viability of the Peyer's patches, mesenteric lymph nodes, and SP cells was 98% and that of the LP lymphocytes was 95%.

Culture Conditions for the Analysis of Cytokine Production

LP and SP T cells from $CR\gamma^{-/Y}$ and control mice were resuspended and cultured in complete medium consisting of RPMI 1640 supplemented with 3 mmol/L L-glutamine, 10 mmol/L HEPES buffer, 10 μg/mL gentamicin, 100 U/mL penicillin and 100 μg/mL streptomycin, 0.05 mmol/L 2-mercaptoethanol, and 10% fetal calf serum (Hyclone Co, Salt Lake City, UT) for the assessment of Th1 and Th2 cytokine synthesis.[4,14,15] For measurement of TGF-β production, serum-free media supplemented with 1% Nutridoma-SP (Boehringer Mannheim Biochemicals, Indianapolis, IN) were used.[28] For the analysis of spontaneous cytokine production, purified LP or SP T cells (1×10^6 cells/mL) were added to culture wells (24-well Costar plates) without exogenous stimulation and cultured for 48 hours (Th1 and Th2 cytokine) and 60 hours (TGF-β).[28] The culture supernatants were then harvested and assayed by cytokine-specific enzyme-linked immunosorbent assay (ELISA) by using the Biotrak IFN-γ, IL-2, IL-4, IL-5, IL-6, IL-12, tumor necrosis factor (TNF)-α ELISA system (Amersham Pharmacia Biotech, Aylesbury, England) and Predica TGF-β ELISA system (Genzyme Corp, Cambridge, MA) according to the manufacturer's protocol. Detection levels of these cytokines were 37–3000 pg/mL for IFN-γ, 34–850 pg/mL for IL-2, 15–375 pg/mL for IL-4, 20–320 pg/mL for IL-5, 50–2000 pg/mL for IL-6, 47–3000 pg/mL for IL-12, 50–2450 pg/mL for TNF-α, and 31.2–2000 pg/mL for TGF-β.

Flow Cytometric Analysis and Cell Sorting

Immunofluorescent analysis was performed using FACScan flow cytometry (Becton Dickinson, Mountain View, CA). Cells stained with single-color reagent were used to set the appropriate compensation levels, and at least 10,000 events were analyzed. Cell sorting was performed on a FACStar (Becton Dickinson). The following monoclonal antibodies (mAbs) from BD PharMingen (San Diego, CA) were used: anti-CD4 (clone RM4-5), anti-CD8 (53-6.7), anti-CD3ε (145-2C11), anti-CD45R/B220 (RA3-6B2), anti-CD11b (M1/70), anti-TCRβ (H57-597), anti-TCRδ (GL3), anti-TCR Vβ2 (B20.6), anti-TCR Vβ3 (KJ25), anti-TCR Vβ4 (KT4), anti-TCR Vβ5.1/5.2 (MR9-4), anti-TCR Vβ6 (RR4-7), anti-TCR Vβ7 (TR310), anti-TCR Vβ8.1/8.2 (MR5-2), anti-TCR Vβ8.3 (1B3.3), anti-TCR Vβ9 (MR10-2), anti-TCR $V\beta10^b$ (B21.5), anti-TCR Vβ11 (RR3-15), anti-TCR Vβ12 (MR11-1), anti-TCR Vβ13 (MR12-3), and anti-TCR Vβ14 (14-2).

For 2-color flow cytometry, 1×10^6 cells in 20 μL phosphate-buffered saline (PBS) containing 2% fetal calf serum and 0.02% sodium azide were first incubated with anti-Fc receptor

mAb (BD PharMingen) to prevent nonspecific staining and then stained with the appropriate fluorescein isothiocyanate (FITC)-conjugated mAb, phycoerythrin (PE)-conjugated mAb, and/or biotinylated mAb followed by streptavidin-phycoerythrin (BD PharMingen). All mAbs were used at the saturating concentrations recommended by the manufacturer.

Staining of intracellular cytokines was performed in accordance with a modified version of the manufacturer's protocol for Fix & Perm Cell Permeabilization Kits (Caltag Laboratories, Vienna, Austria) using the following monoclonal antibodies: FITC/anti-CD11b, FITC/anti-CD4, PE/anti–IL-6, and PE/anti–IFN-γ (BD PharMingen).[29] Negative control samples were stained with irrelevant, isotype-matched PE-conjugated rat IgG1 antibody.

Quantitative Reverse-Transcription PCR

A highly sensitive, quantitative RT-PCR was performed to analyze the IL-6 receptor (IL-6R)– and the antiapoptotic gene (Bcl-x and Bcl-2)-specific mRNA expressions by $CD4^+$ T cells isolated from the colonic LP of diseased $CR\gamma^{-/Y}$ mice.[30] Total RNA was extracted from fluorescence-activated cell sorter (FACS)-purified $CD4^+$ T cells by using TRIzol reagent (Invitrogen, Carlsbad, CA). The RNA was reverse transcribed into complementary DNA (cDNA) using Superscript II reverse transcriptase (Invitrogen), ribonuclease inhibitor (Toyobo, Tokyo, Japan), oligo(dT)12–18 primer (Invitrogen), and deoxyribonucleoside IL-6R mAb (kindly provided by Chugai Pharmaceuticals Co, Ltd, Tokyo, Japan) triphosphates (Amersham Pharmacia Biotech, Arlington Heights, IL). The mixture was incubated at 42°C for 120 minutes and heated to 90°C for 5 minutes. After treatment with ribonuclease H (Toyobo), the synthesized cDNA was extracted by phenol/chloroform. Then, the IL-6R– and the antiapoptotic gene (Bcl-x and Bcl-2)-specific cDNA were quantified using LightCycler-DNA Master Hybridization Probes (Roche Diagnosis, Mannheim, Germany). For the amplification of cDNA, 20 μL of the PCR mix was added to each tube to give a final concentration of 0.05 μmol/L 5′ primer, 0.05 μmol/L 3′ primer, 0.2 μmol/L FITC-labeled probe, 0.2 μmol/L LightCycler Red 640 (LCR)-labeled probe, 2 mmol/L $MgCl_2$, and 1 × LightCycler-DNA Master Hybridization Probes mix (Roche Diagnosis). We used the oligo primers specific for IL-6R (sense, 5′-AAGAGTGACTTCCAGGTGCC-3′; antisense, 5′-GGTATCGGAAGCTGGAACTGC-3′), Bcl-x (sense, 5′-TGGTCGACTTTCTCTCCTAC-3′; antisense, 5′-GAGATCCACAAAAGTGTCCC-3′), Bcl-2 (sense, 5′-TGCACCTGACGCCCTTCAC-3′; antisense, 5′-TAGCTGATTCGACCATT TGCCTGA-3′), and glyceraldehyde-3-phosphate dehydrogenase (GAPDH) (sense, 5′-TTCACCACCATGGAGAAGGC-3′; antisense, 5′-GGCATGGACTGTGGTCATGA-3′). To detect the target molecule, we then followed the manufacturer's protocol to prepare an FITC-labeled hybrid probe and an LCR-labeled hybrid probe to IL-6R (FITC, 5′-TGATACCACAAGGTTGGCAGGTGG-3′; LCR, 5′-TCCGGCTGCACCATTTTTAAGCTG-3′), Bcl-x (FITC, 5′-CTCTTTCGGGATGGAGTAAACTGGGG-3′; LCR, 5′-CGCATCGTGGCCTTTTTCTCCTT-3′), Bcl-2 (FITC, 5′-CCCTGTTGACGCTCTCCACACACA-3′; LCR, 5′-GACCCCACCGAACTCAAAGAAGGC-3′), and GAPDH (FITC, 5′-TGGG TGTGAACCACCAGAAATATGAC-3′; LCR, 5′-ACTCACTCAAGATTGTCAGCAATGCA-3′). After heating at 94°C for 2 minutes, cDNA were amplified for 40 cycles, with each cycle consisting of 95°C for 10 seconds, 55°C for 30 seconds, and 72°C for 30 seconds. Once during the cycle the log-linear signal could be distinguished from the background, it was then possible to compare the target concentrations (external standard) in samples with an internal standard in the same samples. After the PCR had been completed, the LightCycler software (Roche Diagnosis) automatically converted the raw data into copies of target molecules. In this study, the relative quantitative expression of IL-6R–, Bcl-x–, or Bcl-2–specific mRNA in each sample was expressed as the quantity of the respective mRNA divided by the quantity of mRNA GAPDH.[30]

Treatment of Mice With Anti–IL-6R mAb

Rat IgG anti-mouse IL-6R mAb[31] or isotype-matched rat IgG (BD PharMingen) at a dose of 8 mg per mouse was injected intraperitoneally into euthymic (nu/+) mutant $CR\gamma^{-/Y}$ mice at the age of 6 weeks. The weekly mAb treatment was continued for 4 weeks. Rat anti-mouse IL-6R mAb was prepared from the MR16-1 hybridoma cell line according to the protocol previously described elsewhere.[31]

Analysis of Apoptosis Following Anti–IL-6R mAb Treatment

To examine the effect of anti–IL-6R mAb for the induction of apoptosis in IL-6–producing $CD4^+$ T cells from $CR\gamma^{-/Y}$ mice, a previously established in vitro apoptosis analysis protocol was used.[32] Thus, SP and colonic LP $CD4^+$ T cells were isolated from $CR\gamma^{-/Y}$ mice and then cocultured with anti–IL-6R mAb (1 mg/mL, MR16-1) or isotype control IgG (BD PharMingen) for 6 hours. $CD4^+$ T cells were harvested for FACS analysis using the Annexin V FITC Apoptosis Detection Kit I (BD PharMingen).[32]

Adoptive Transfer Experiment

SP cells were aseptically removed from euthymic (nu/+) mutant $CR\gamma^{-/Y}$ donor mice with colitis. Erythrocytes were removed by hypotonic lysis. To avoid stimulating T cells during the purification process, a negative selection procedure was used for the preparation of $CD4^+$ T cells. Initially, mononuclear cells were resuspended in complete medium and then incubated in culture plates (Millipore, Bedford, MA) for 2 hours at 37°C to remove adherent cells, including macrophages and fibroblasts.[33] The nonadherent cell suspension was then incubated in wells precoated with $F(ab')_2$ fragments of goat anti-mouse IgG (Jackson, West Grove, PA) at 4°C for 90 minutes.[33] To obtain the T-cell–enriched fraction, wells were washed gently 3 times with PBS containing 5% fetal calf serum. The T-cell–enriched fraction was then subjected to magnetic-activated cell sorting (Miltenyi Biotec, Gladbach, Germany) with anti-CD4–coated beads (Miltenyi Biotec) for

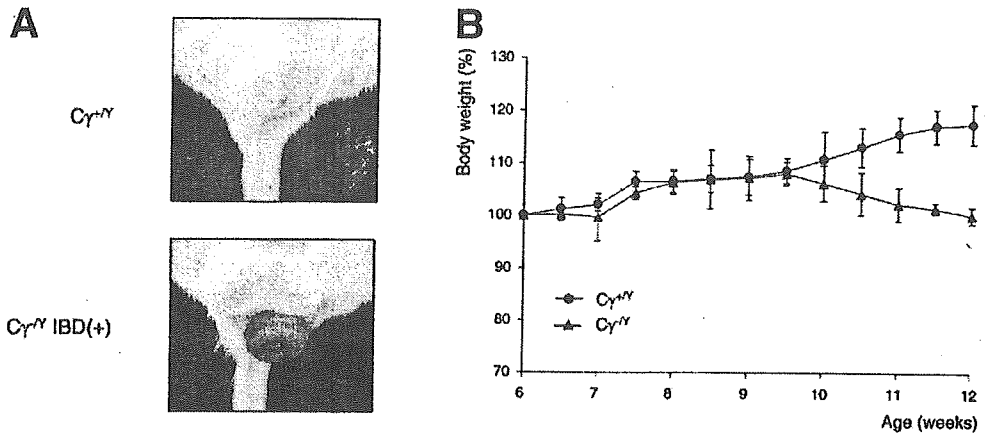

Figure 1. Gross appearance of the (*A*) anorectal prolapse and (*B*) body weight changes in CRγ$^{+/Y}$ mice, CRγ$^{-/Y}$ mice without IBD, and CRγ$^{-/Y}$mice with IBD. CRγ$^{-/Y}$ mice with IBD showed anal prolapse beginning at 8 weeks of age and obvious lack of body weight gain from 10 weeks of age. The data represent the values (mean ± SD) from 3 different experiments (4 mice per group).

preparation of CD4$^+$ T cells.[34] The purified donor CD4$^+$ T cells (3×10^6) were resuspended in sterile PBS and injected intraperitoneally (1 mL) into C.B-17 SCID mice (Clea Japan). Five weeks after the adoptive transfer, mice were examined for the presence of disease.

Histologic Analysis

Small and large intestines obtained from CRγ$^{-/Y}$ and control mice at predetermined time points were fixed in 4% paraformaldehyde in PBS for 4 hours and embedded in paraffin for the preparation of 5-μm tissue sections. The sections were stained with H&E for the assessment of disease and clinical score. Periodic acid–Schiff/alcian blue staining was performed for the identification of goblet cells.

Assessment of Disease Score

Histopathologic alterations in the colon were semi-quantified according to a modified scoring system[35] using the following criteria: (1) cellular infiltration into the lamina propria of the large intestine (score from 0 to 3), (2) mucin depletion (score from 0 to 2), (3) crypt abscesses (score from 0 to 2), (4) epithelial erosion (score from 0 to 2), (5) hyperemia (score from 0 to 3), and (6) thickness of the

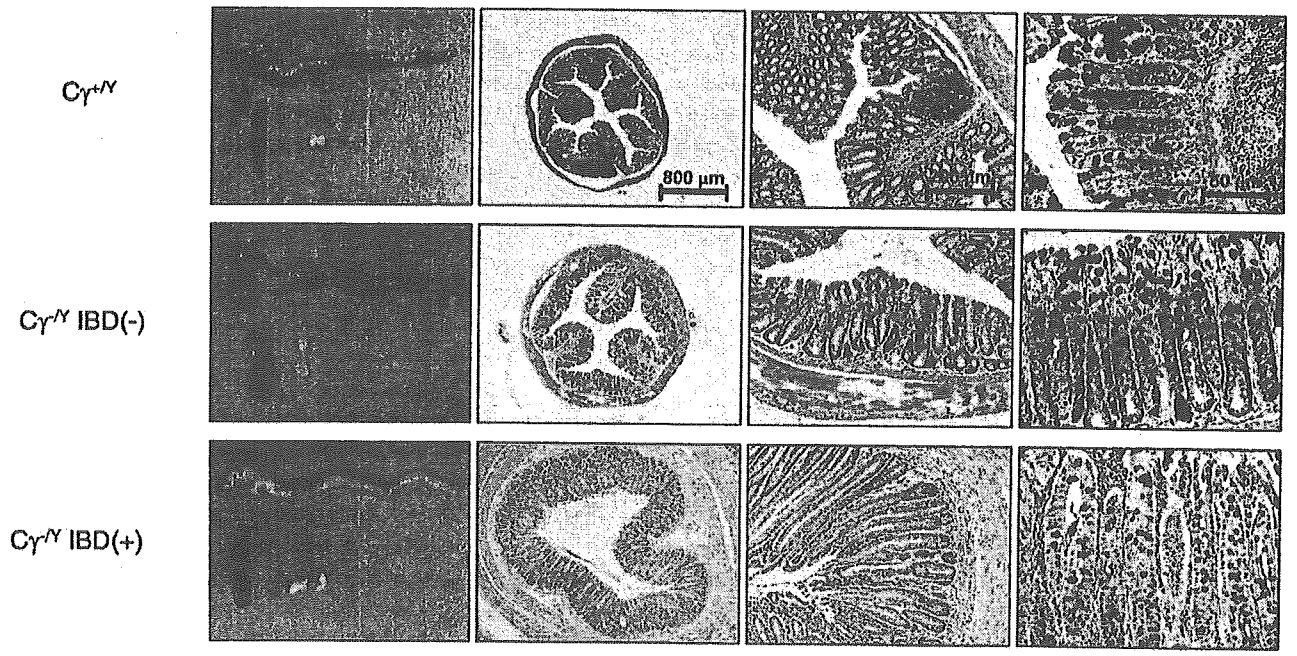

Figure 2. Macroscopic and microscopic appearance of the large intestine in CRγ$^{+/Y}$ mice, CRγ$^{-/Y}$ mice without IBD, and CRγ$^{-/Y}$ mice with IBD. The large intestine of the mice was dissected for routine histologic analysis, including fixing with 4% paraformaldehyde, embedding in paraffin, and staining with H&E. Histopathologic alteration in the colons was assessed by use of a modified clinical analysis system.

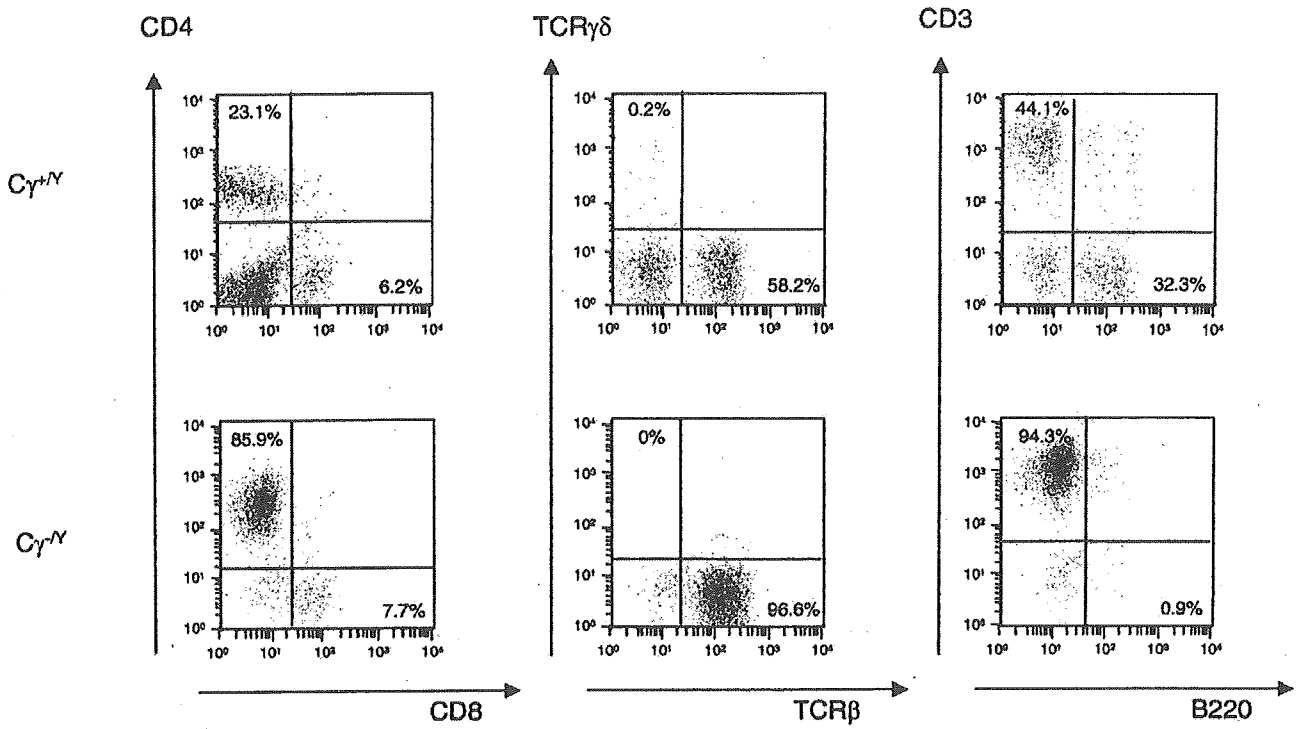

Figure 3. Flow cytometric analysis of colonic LP lymphocytes isolated from CRγ$^{-/Y}$ and CRγ$^{+/Y}$ mice. CRγ$^{-/Y}$ mice did not possess mature B cells or TCR γδ T cells but had increased numbers of CD4$^+$ T cells. The data are representative of results from 2 independent experiments.

colonic mucosa (score from 1 to 3). Hence, the range of histopathologic scores was from 1 (no alteration) to 15 (most severe colitis).

Statistical Analysis

Significant differences between mean values were determined by use of the Student *t* test. *P* values of .05 were considered statistically significant.

Results

Histologic Appearance of Colonic Inflammation in Euthymic (nu/+) Mutant CRγ$^{-/Y}$ Mice

At 8 weeks of age, all of the euthymic (nu/+) mutant CRγ$^{-/Y}$ mice developed signs of IBD, characterized by anorectal prolapse (Figure 1*A*), lack of weight gain (Figure 1*B*), and a hunched posture. Necropsy of the diseased euthymic (nu/+) mutant CRγ$^{-/Y}$ mice revealed inflammation of the large intestine and rectum and a more marked hyperplasia, dilatation, and thickening of the wall than seen in control euthymic (nu/+) wild-type CRγ$^{+/Y}$ mice and euthymic (nu/+) mutant CRγ$^{-/Y}$ mice without IBD (Figure 2). In addition, microscopic examination of the diseased euthymic (nu/+) mutant CRγ$^{-/Y}$ mice revealed elongation, hyperemia, crypt distortion, goblet cell reduction, and lymphocyte infiltration into the colonic lamina propria (Figure 2).

Cell Population of Euthymic (nu/+) Mutant CRγ$^{-/Y}$ Mice

Lack of functional CRγ has been reported to affect lymphocyte development.[22–26] In both young adult and aged CRγ$^{-/Y}$ mice, we noted the absence of natural killer cells (data not shown) and γδ T cells and a great reduction in B cells (Figure 3). Among lymphocytes isolated from colonic LP of 8-week-old CRγ$^{-/Y}$ mice, we found that increased numbers of CD4$^+$ T cells but not of CD8$^+$ T cells (Figure 3) were always associated with colitis.

TCR Vβ Repertoire Use of Colonic LP CD4$^+$ T Cells by Euthymic (nu/+) Mutant CRγ$^{-/Y}$ Mice With Colitis

Because the increase of LP CD4$^+$ T cells was associated with development of colitis, we next analyzed the qualitative alterations in the CD4$^+$ T cells. Flow cytometric analysis of TCR Vβ repertoire use in colonic LP CD4$^+$ T cells isolated from euthymic (nu/+) wild-type CRγ$^{+/Y}$ and euthymic (nu/+) mutant CRγ$^{-/Y}$ mice without IBD showed that the major TCR Vβ repertoire use was TCR Vβ8, followed by Vβ4, Vβ6, and Vβ14 (Figure 4). In contrast, CD4$^+$ T cells isolated from

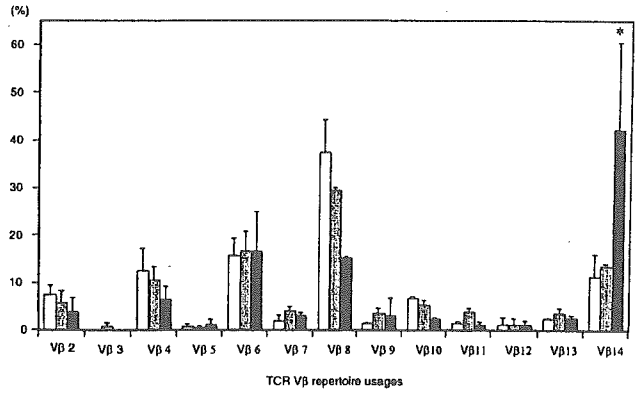

Figure 4. Flow cytometric analysis of the TCR Vβ repertoire of CD4+ T cells isolated from colonic LP of the CRγ$^{-/Y}$ and CRγ$^{+/Y}$ mice. Mononuclear cells isolated from CRγ$^{-/Y}$ mice with or without colitis and control CRγ$^{+/Y}$ mice were costained with mAbs specific for FITC/TCR Vβ and PE/CD4. The percentage of T cells bearing each TCR Vβ was calculated as 100 × (% of CD4+, Vβx+ cells)/(% of CD4+ cells). The percentages of T cells are expressed as the mean values from 3 different mice. *White, dotted,* and *black bars* represent CRγ$^{+/Y}$ mice, CRγ$^{-/Y}$ mice without IBD, and CRγ$^{-/Y}$ mice with IBD, respectively. Statistical comparisons were determined by Student *t* test (*$P < .05$).

euthymic (nu/+) mutant CRγ$^{-/Y}$ mice with IBD had a predominance of TCR Vβ14 (Figure 4). Further, under immunoscope analysis of CDR3 length to investigate the clonality of these Vβ14+ T cells, Gaussian distribution of clonotype was observed, suggesting the polyclonality of colonic CD4+ T cells in the diseased mice (data not shown). Thus, local augmentation of CD4+ T cell populations expressing TCR Vβ14 was associated with the development of colitis in the CRγ$^{-/Y}$ mice.

Characterization of IL-6–Producing LP CD4+ T Cells Isolated From Euthymic (nu/+) Mutant CRγ$^{-/Y}$ Mice With Colitis

We next examined the ability of the CD4+ T cells in colonic LP of euthymic (nu/+) mutant CRγ$^{-/Y}$ mice with IBD to produce Th1- or Th2-type cytokines. LP lymphocytes were isolated from young, anal prolapse–free (6 weeks of age) and diseased (8–12 weeks) mice. The cells were cultured in complete medium without exogenous stimulation to determine their spontaneous cytokine production. Minimum amounts of IL-6 (376 ± 3 pg per 10^6 cells) were detected in the culture supernatants harvested from the wells containing colonic LP lymphocytes of young healthy CRγ$^{-/Y}$ mice. The level of spontaneous IL-6 production was increased in the various stages of colitis from 375.9 ± 3.3 pg per 10^6 cells in the anal prolapse–free mice to 2655.1 ± 410.4 pg per 10^6 cells in the diseased mice (Figure 5). When cytokine production was examined, these colonic CD4+ T cells did not produce IL-4, IL-5, IL-12, and TNF-α. Although IFN-γ was noted in the culture containing colonic CD4+

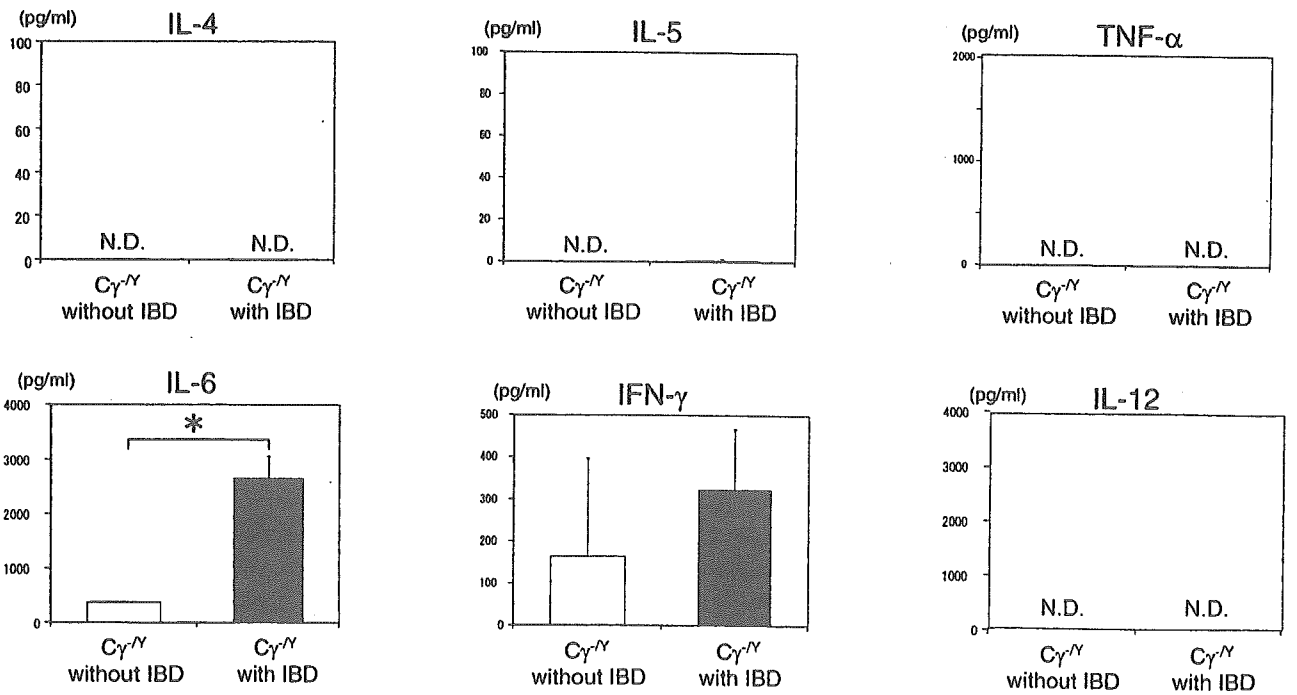

Figure 5. Analysis of cytokine production expression by colonic CD4+ T cells isolated from CRγ$^{-/Y}$ mice with (*closed squares*) and without (*open squares*) IBD. Whole colonic LP mononuclear cells were incubated in complete medium with 10% fetal calf serum for 48 hours without any exogenous stimulation. The culture supernatants were harvested for cytokine-specific ELISA. The data represent the mean ± SD from 3 different experiments. Statistical comparisons were determined by Student *t* test (*$P < .05$).

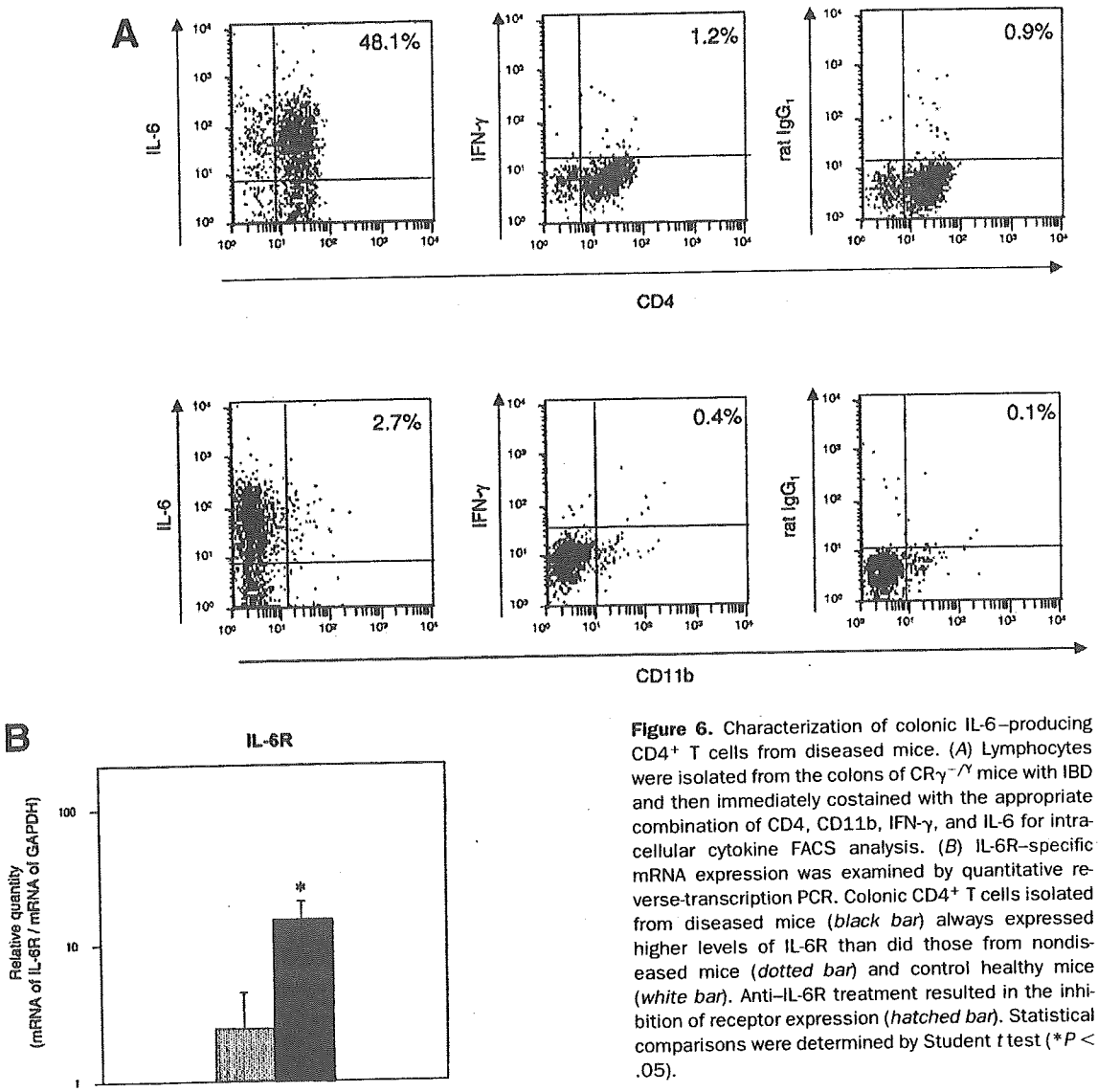

Figure 6. Characterization of colonic IL-6–producing $CD4^+$ T cells from diseased mice. (*A*) Lymphocytes were isolated from the colons of $CR\gamma^{-/Y}$ mice with IBD and then immediately costained with the appropriate combination of CD4, CD11b, IFN-γ, and IL-6 for intracellular cytokine FACS analysis. (*B*) IL-6R–specific mRNA expression was examined by quantitative reverse-transcription PCR. Colonic $CD4^+$ T cells isolated from diseased mice (*black bar*) always expressed higher levels of IL-6R than did those from nondiseased mice (*dotted bar*) and control healthy mice (*white bar*). Anti–IL-6R treatment resulted in the inhibition of receptor expression (*hatched bar*). Statistical comparisons were determined by Student *t* test (*$P <$ .05).

T cells, the level of production was not statistically different from $CD4^+$ T cells isolated from nondiseased mice.

To directly show IL-6 production by colonic LP $CD4^+$ T cells from euthymic (nu/+) mutant $CR\gamma^{-/Y}$ mice with colitis, we next performed intracellular cytokine FACS analysis of such cells. The results obtained by double staining with appropriate fluorescence-conjugated mAb anti-CD4, anti-CD11b, and anti–IL-6 showed that IL-6 was mainly produced by $CD4^+$ T cells but not by CD11b-positive cells (Figure 6*A*). Once we knew that these colonic $CD4^+$ T cells preferentially produce IL-6, we next sought to examine whether these T cells express IL-6R. When IL-6R–specific mRNA expression was examined by quantitative reverse-transcription PCR, colonic $CD4^+$ T cells isolated from the diseased mice always expressed higher levels of the IL-6R message than did those from nondiseased mice (Figure 6*B*). These findings suggest that the increase in pathogenic $CD4^+$ T cells in the large intestine of diseased mice may result from the creation of autocrine-induced antiapoptotic conditions by IL-6 and IL-6R.

Efficacy of In Vivo Treatment With Anti–IL-6R mAb

We next conducted further experiments to confirm our findings that $CD4^+$ Th-cell–derived IL-6 was implicated in the development of colitis. Thus, young adult mice without clinical signs of the disease were treated with anti–IL-6R mAb, mock antibody, or PBS. Like untreated mice, mice treated with the mock antibody or PBS devel-